

Supramolecular Structures from Rod–Coil Block Copolymers

Myongsoo Lee,^{*,†} Byoung-Ki Cho,[†] and Wang-Cheol Zin[‡]

Department of Chemistry, Yonsei University, Shinchon 134, Seoul 120-749, Korea, and Department of Materials Science and Engineering and Polymer Research Institute, Pohang University of Science and Technology, Pohang 790-784, Korea

Received February 22, 2001

Contents

I. Introduction	3869
II. Rod–Coil Block Copolymer Theories	3869
III. Rod–Coil Copolymers Based on Helical Rods	3872
IV. Rod–Coil Copolymers Based on Mesogenic Rods	3875
A. Bulk-State Supramolecular Structures	3875
B. Supramolecular Structures from Binary Mixtures	3882
V. Rod–Coil Copolymers Based on Conjugated Rods	3884
VI. Conclusions	3890
VII. Acknowledgments	3891
VIII. References	3891

I. Introduction

One of the fascinating subjects in areas such as materials science, nanochemistry, and biomimetic chemistry is concerned with the creation of supramolecular architectures with well-defined shapes and functions. Self-assembly of molecules through non-covalent forces including hydrophobic and hydrophilic effects, electrostatic interactions, hydrogen bonding, microphase segregation, and shape effects has the great potential for creating such supramolecular structures.^{1–5} An example is provided by rodlike macromolecules whose solutions and melts exhibit liquid crystalline phases such as nematic and/or layered smectic structures with the molecules arranged with their long axes nearly parallel to each other.^{6,7} The main factor governing the geometry of the supramolecular structures in the liquid crystalline phase is the anisotropic aggregation of the molecules. In contrast, coil–coil diblock molecules consisting of different immiscible segments exhibit a wide range of microphase-separated supramolecular structures with curved interfaces in addition to layered structures.^{8–11} This phase behavior is mainly due to the mutual repulsion of the dissimilar blocks and the packing constraints imposed by the connectivity of each block.

The covalent linkage of these different classes of molecules to a single linear polymer chain (rod–coil copolymer) can produce a novel class of self-assembling materials since the molecules share certain general characteristics of diblock molecules and rodlike liquid crystalline molecules.^{12–15} The difference

in chain rigidity of stiff rodlike and flexible coillike block is expected to greatly affect the details of molecular packing and thus the nature of thermodynamically stable supramolecular structures. This rod–coil molecular architecture imparts microphase separation of the rod and coil blocks into ordered periodic structures even at very low molecular weights relative to flexible block copolymers due to the high stiffness difference between the blocks. As a consequence, the rod–coil copolymer forms supramolecular structures with dimensions as small as few nanometers, which are not common in microphase-separated flexible block copolymers.¹⁶ The supramolecular structures of rod–coil polymers arise from a combination of organizing forces including the mutual repulsion of the dissimilar blocks and the packing constraints imposed by the connectivity of each block, and the tendency of the rod block to form orientational order. Apart from the wide range of different supramolecular structures in nanoscale dimensions, another unique characteristic is that rod segments can endow various functionalities such as photophysical and electrochemical properties to the supramolecular materials.

Many of the syntheses of rod–coil diblock and triblock copolymers as well as their interesting supramolecular structures and the intriguing properties of rod–coil copolymers are discussed in excellent books and reviews that have been published by several experts in the field.^{16–19} Here, we do not want to present a complete overview on reported rod–coil copolymers. Instead, we have highlighted the most recently synthesized rod–coil copolymers and their supramolecular structures.

II. Rod–Coil Block Copolymer Theories

In A-B diblock copolymers with well-defined molecular architectures, microphase separation occurs, and microdomains rich in monomer A and in monomer B are formed. When microphase separation occurs, the microdomains are not dispersed randomly but form a rather regular arrangement giving rise to a periodic structure. The geometry of the microdomain is largely dictated by the relative volume fraction of the A block to that of the B block.^{8–11,20–23} Conformational asymmetry between A and B blocks also plays a significant role in determining the geometry of the lattice. Several theoretical attempts have been made to deal with this conformational asymmetry and study its effects on the microphase-separated morphologies.^{24–27} Increasing the chain stiffness of a polymer chain eventually results in a rodlike block that can be characterized by a persis-

* To whom correspondence should be addressed. FAX: 82-2-364-7050. E-mail: mslee@yonsei.ac.kr.

[†] Yonsei University.

[‡] Pohang University of Science and Technology.



Myongsoo Lee, born in 1960, received a bachelor degree in Chemistry from Chungnam National University, Korea, in 1982 and his Ph.D. degree in Macromolecular Science from Case Western Reserve University, Cleveland, in 1992. In the same year, he became a postdoctoral fellow at University of Illinois, Urbana-Champaign. In 1993, he was a senior research scientist at Korea Research Institute of Chemical Technology where he worked in the field of π -conjugated systems. In 1994, he joined the Faculty of Chemistry at Yonsei University, Korea, where he is presently Associate Professor of Chemistry. His current research interests include synthetic self-organizing macromolecules, controlled supramolecular architectures, and organic nanostructured materials.



Byoung-Ki Cho was born in Daejeon, Korea, in 1971 and studied Chemistry at Yonsei University, Korea. After receiving his B.S. degree in 1996, he joined the research group of Professor Myongsoo Lee, Yonsei University, where he received his Ph.D. degree in 2001. His graduate research focused on supramolecular organization based on organic rod building blocks. During his graduate study, he received research excellence award in Yonsei University and graduate fellowship granted by Seo-Am Foundation. Dr. Cho is currently a postdoctoral associate at Cornell University, Ithaca.

tent length and whose end to end distance scales linearly with the number of monomer units.

Rod-coil block copolymers have both rigid rod and block copolymer characteristics. The formation of liquid crystalline nematic phase is characteristic of rigid rod, and the formation of various nanosized structures is a block copolymer characteristic. A theory for the nematic ordering of rigid rods in a solution has been initiated by Onsager and Flory,^{28,29} and the fundamentals of liquid crystals have been reviewed in books.^{30,31} The theoretical study of coil-coil block copolymer was initiated by Meier,³² and the various geometries of microdomains and micro phase transitions are now fully understood. A phase diagram for a structurally symmetric coil-coil block copolymer has been theoretically predicted as a



Wang-Cheol Zin received his Ph.D. degree from the University of Cincinnati in 1983 and did postdoctoral work at Stanford University before joining the Korea Research Institute of Chemical Technology as a senior researcher. He is Professor of Materials Science and Engineering at the Pohang University of Science and Technology since 1986. His research focuses on the self-organization of rod-coil block molecules and phase relationship in block copolymers and polymer blends.

function of the volume fraction of one component f and the product χN , where χ is the Flory-Huggins interaction parameter and N is the degree of polymerization.³³ A predicted stable microstructure includes lamellae, hexagonally packed cylinders, body-centered cubic spheres, close-packed spheres, and bicontinuous cubic network phases with $Ia\bar{3}d$ symmetry (Figure 1).

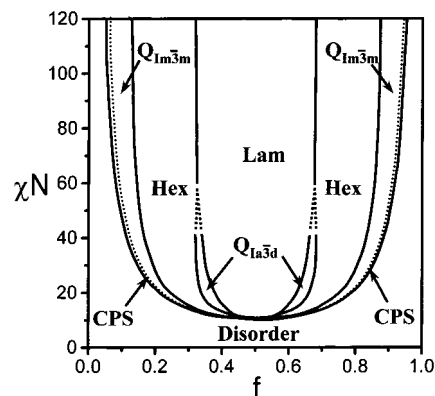


Figure 1. Phase diagram for a structurally symmetric coil-coil block copolymer (Lam = lamellae, Hex = hexagonally packed cylinders, $Q_{Ia\bar{3}d}$ = bicontinuous cubic with $Ia\bar{3}d$ symmetry, $Q_{Im\bar{3}m}$ = body-centered cubic, CPS = close packed sphere).

Including both rod and block characters, Semenov and Vasilenko (SV) have initiated a theoretical study on the phase behavior of rod-coil block copolymers.¹² In their study, SV only considered the nematic phase and smectic A lamellar phases where rods remain perpendicular to the lamellae. The smectic phase has either a monolayer or bilayer structure. In the following study, Semenov included the smectic C phases, where the rods are tilted by an angle θ to the lamellar normal.^{13,14} The model also included a weak phase in which lamellar sheets containing the rigid rod were partly filled by flexible coil. For free energy calculations, SV introduced four main terms: ideal gas entropy of mixing, steric interaction among rods, coil stretching, and unfavorable rod-coil interactions. The ideal gas entropy of the mixing term is

associated with the spatial placement of the junction point of rod–coil molecules. To find the steric interaction energy term of the rods SV used the lattice packing model (Flory lattice approach). Coil stretching arises from the constraint of the density uniformity, and it restricts the number of possible conformations of flexible coil in the structured system. The Flory–Huggins interaction parameter measures unfavorable rod–coil interaction energy. The schematic phase diagram calculated shows various phases as a function of the volume fraction of the flexible component f , the product χN and the ratio ν of the characteristic coil to rod dimensions. In rod–coil block copolymers, the shape of the phase diagram is affected by the ratio ν . It was also shown that the nematic–smectic transition is a first-order transition, while the smectic A–smectic C transition is a continuous second-order transition.

Williams and Fredrickson proposed the hockey puck micelle (one of the nonlamellar structure) where the rods are packed axially to form finite-sized cylindrical disk covered by coils (Figure 2).¹⁵ They

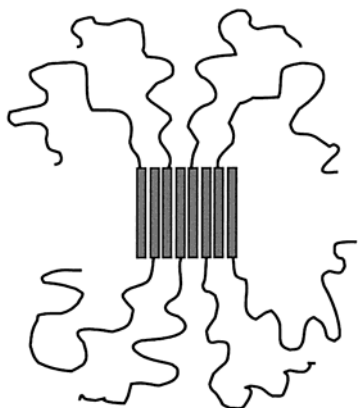


Figure 2. Schematic representation of a monolayer puck.

predicted that the hockey puck structure should be stable at large coil fractions ($f > 0.9$). The main advantage of micelle formation relative to lamellae is the reduction of the stretching penalty of coils; because in a rod–coil block copolymer the coils are permanently attached to the rods, complete separation is never possible, and there is always some interface between the two. In general, the sharper the interface, the more the coils have to stretch and the greater the stretching free energy. At high χ values, the system can be modeled as a set of chains grafted to a wall. In the lamellae structure, the highly grafted chains pay a large stretching penalty. This penalty is governed by how rapidly the volume away from the interface increases. In a micellar puck, the rods are assumed to be well aligned to get rid of the strong steric problems, and the chains are assumed to form a hemispherical shell at a radius of R from the disk with a constant surface density on this shell. The coils are strongly stretched inside the hemisphere. The model assumed that coils travel in straight line trajectories, consistent with constant density constraints. After the chains have passed this hemisphere, they are assumed to have radial trajectories as if they emanated from the center of the puck. This model has only one free parameter R to

minimize free energy. The main disadvantage of forming the hockey puck relative to lamellae is the creation of an extra surface, for which they pay a surface energy penalty. WF, following the SV approach, included the hockey puck micelle phase in the phase diagram by comparing the free energy of micelle to that of the lamellar structures (Figure 3).

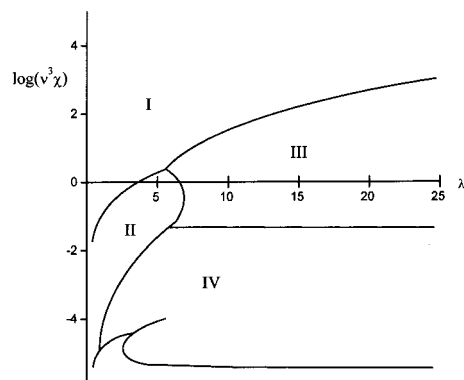
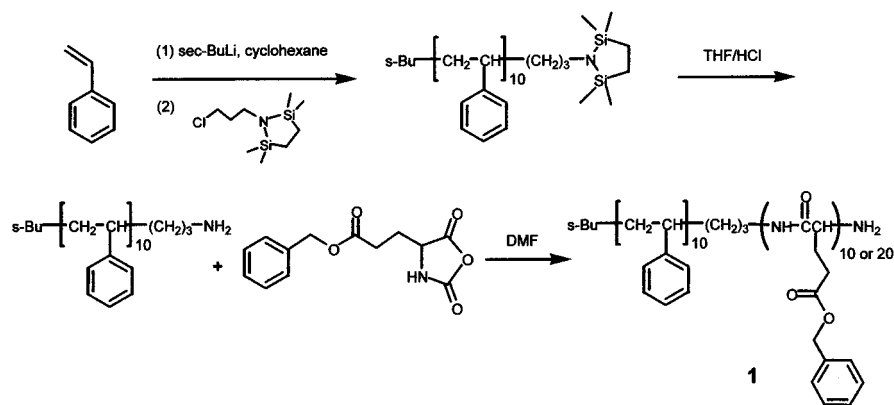


Figure 3. Phase diagram including the hockey puck and lamellae phases. The phases are (I) bilayer lamellae, (II) monolayer lamellae, (III) bilayer hockey pucks, (IV) monolayer hockey pucks, and (V) incomplete monolayer lamellae. $\text{Log}(v^3\chi)$ is plotted against λ . $\lambda = \phi/(1 - \phi)$ where ϕ is the volume fraction of the coil. $\nu = \kappa/\lambda$ and $\kappa = Na^2/L^2$ where the coil part is assumed to consist of N segments with a mean-square separation between adjacent segments of $6a^2$, and L is the rod length. χ is the Flory–Huggins interaction parameter.

Müller and Schick (MS) studied the phase behavior of rod–coil molecules by applying the numerical self-consistent field theory within the weak segregation limit.³⁴ In the strong segregation limit at high incompatibilities, MS used a brush-like approximation to determine the phase boundaries. Their most interesting finding was that in stable morphologies the coils are on the convex side of the rod–coil interface. This result emphasizes the importance of the conformational entropy of the flexible component, which is increased when the coil occupies the larger space on the convex side of the interface. They also found that the extreme structural asymmetry in rod–coil blocks has a pronounced influence on the phase diagram. The wide region encompassing cylinder phase was also predicted in the phase diagram of a rod–coil block copolymer in the weak segregation limit. Matsen and Barrett also applied the self-consistent field techniques to the SV model for lamellar structures.³⁵ Their theory predicts a nematic phase composed by the mixing of rods and coils when $\chi N < 5$. By increasing χN , the various lamellar phases appear as a stable phase.

Scaling approaches have been used to theoretically predict the structures of rod–coil block molecules in a selective solvent.^{36–38} Halperin investigated the transition between smectic A and smectic C by comparing interfacial and coil deformation free energy. Since the tilt increases the surface area per coil, tilting is favored when the stretching penalty of the coil is dominant. At high f , the suggested shape of the stable micelle was similar to hockey puck structure presented by WF. In addition, Raphael and de Gennes suggested “needles” and “fence” morphologies

Scheme 1



of coil–rod–coil triblock copolymers in a selective solvent of low molecular weight.

III. Rod–Coil Copolymers Based on Helical Rods

Polymers with a stiff helical rodlike structure have many advantages over other synthetic polymers because they possess stable secondary structures due to cooperative intermolecular interactions. An example of polymers with helical conformation is polypeptides in which the two major structures include α -helices and β -sheets. The α -helical secondary structure enforces a rodlike structure, in which the polypeptide main chain is coiled and forms the inner part of the rod.¹⁸ This rodlike feature is responsible for the formation of the thermotropic and lyotropic liquid crystalline phases. Polypeptide molecules with α -helical conformation in the solution are arranged with their long axes parallel to each other to give rise to a nematic liquid crystalline phase. However, even long chain polypeptides can exhibit a layered supramolecular structure, when they have a well-defined chain length. For example, the monodisperse poly(α ,L-glutamic acid) prepared by the bacterial synthetic method assembles into smectic ordering on length scales of tens of nanometers.^{39,40}

Incorporation of an elongated coillike block to this helical rod system in a single molecular architecture may be an attractive way of creating new supramolecular structures due to its ability to segregate incompatible segment of individual molecules. The resulting rod–coil copolymers based on a polypeptide segment may also serve as models providing insight into the ordering of complicated biological systems. High molecular weight rod–coil block copolymers consisting of a polypeptide connected to either a polystyrene or a polybutadiene were thoroughly studied by Gallot et al.^{18,41–43} These rod–coil copolymers were observed to self-assemble into lamellar structures with a uniform thickness even though the polypeptide blocks are not monodisperse. Furthermore, one of these studies that involved hydrophobic–hydrophilic polypeptide rod–coil copolymers with coil volume fractions ranging between approximately 25 and 45% showed that the rods are tilted 15–70° in the lamellae and that the tilt angle increased with water content.⁴³ In all these studies, the polypeptide segments in these block copolymers have an α -helix conformation.

Very recently, low molecular weight block copolymers consisting of poly(γ -benzyl-L-glutamate) with degrees of polymerization of 10 or 20 and polystyrene with degree of polymerization of 10 were synthesized by Klok, Lecommandoux, and a co-worker (Scheme 1).⁴⁴ The coil block was synthesized by conventional living anionic polymerization initiated by *sec*-butyllithium followed by end capping with 1-(3-chloropropyl)-2,2,5,5-tetramethyl-1-aza-2,5-disilacyclopentane. Acid-catalyzed hydrolysis produced a primary amine functionalized oligostyrene with a degree of polymerization of 10. The resulting primary amine functionalized polystyrene was then used as a macroinitiator for the polymerization of γ -benzyl-L-glutamate *N*-carboxyanhydride to produce the polypeptide block. The length of the polypeptide segment was controlled by the molar ratio of the *N*-carboxyanhydride monomer to the primary amine macroinitiator. In this way, two different rod–coil copolymers consisting of polystyrene with the degree of polymerization of 10 and polypeptide containing either 10 or 20 γ -benzyl-L-glutamate repeating units were prepared.

Both the rod–coil polymers were observed to exhibit thermotropic liquid–crystalline phases with assembled structures that differ from the lamellar structures. Incorporation of a polypeptide segment into a polystyrene segment was observed to induce a significant stabilization of the α -helical secondary structure as confirmed by FT-IR spectra. However, small-angle X-ray diffraction patterns indicated that α -helical polypeptides do not seem to assemble into hexagonal packing for the rod–coil copolymer with 10 γ -benzyl-L-glutamate repeating units. The amorphous character of the polystyrene coil is thought to frustrate a regular packing of the α -helical fraction of the short polypeptide segments. Increasing the length of the polypeptide segment to a DP of 20 gives rise to a strong increase in the fraction of diblock copolymers with α -helical polypeptide segment. By studying this block copolymer with small-angle X-ray analysis, a 2-D hexagonal columnar supramolecular structure was observed with a hexagonal packing of the polypeptide segments adopting an 18/5 α -helical conformation with a lattice constant of 16 Å. The authors proposed a packing model for the formation of the “double-hexagonal” organization (Figure 4). In this model, the rod–coil copolymers are assembled

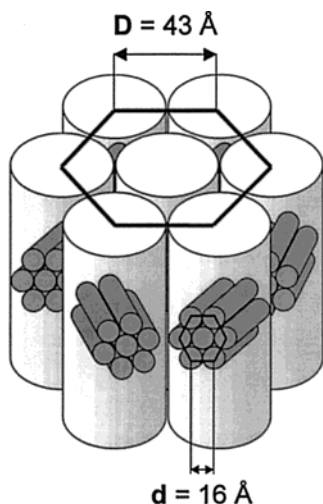


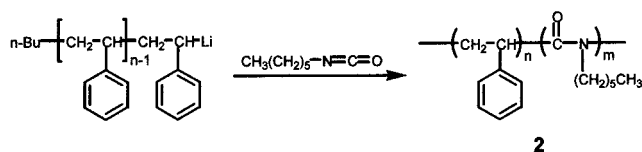
Figure 4. Packing model for the formation of “double-hexagonal” organization. (Reprinted with permission from ref 44. Copyright 2000 American Chemical Society).

in a hexagonal fashion into infinitely long columns, with the polypeptide segments oriented perpendicularly to the director of the columns. The subsequent supramolecular columns are packed in a superlattice with hexagonal periodicity parallel to the α -helical polypeptide segments with a lattice constant of 43 Å.

In contrast to polypeptides that have many possible conformations, poly(hexyl isocyanate) is known to have a stiff rodlike helical conformation in the solid state and in a wide range of solvents, which is responsible for the formation of a nematic liquid crystalline phase.^{45–47} The inherent chain stiffness of this polymer is primarily determined by chemical structure rather than by intramolecular hydrogen bonding. This results in a greater stability in the stiff rodlike characteristics in the solution as compared to polypeptides. The lyotropic liquid crystalline behavior in a number of different solvents was extensively studied by Aharoni et al.^{48–50} In contrast to homopolymers, interesting new supramolecular structures can be expected if a flexible block is connected to the rigid polyisocyanate block (rod–coil copolymers) because the molecule imparts both microphase separation characteristics of the blocks and a tendency of rod segments to form anisotropic order.

Ober and Thomas et al. reported on rod–coil diblock copolymers consisting of poly(hexyl isocyanate) as the rod block and polystyrene as the coil block (Scheme 2).^{51–53} The polymers (**2**) were synthesized

Scheme 2



by sequential living anionic polymerization initiated by *n*-butyllithium. A block copolymer consisting of poly(hexyl isocyanate) with DP of 900 and polystyrene with DP of 300 displays liquid crystalline behavior in concentrated solutions, suggestive of an anisotropic order of rod segments.⁵¹ Transmission electron mi-

croscopy of bulk and thin film samples cast from toluene solutions showed the existence of a zigzag morphology with high degree of smectic-like long-range order. The average domain spacings of the poly(hexyl isocyanate) block are approximately 180 nm and of the polystyrene block approximately 25 nm. Wide-angle electron diffraction pattern showed that the rod domains are highly crystalline with an orientational order. In addition, electron diffraction patterns that showed the orientation of the rod blocks with respect to the zigzags confirmed that the rods are tilted with respect to the interface separating the rod and coil domains. On the basis of these data, the authors proposed a packing model either as an interdigitated model or as a bilayer model (Figure 5). Of the two proposed models for zigzag morphology,

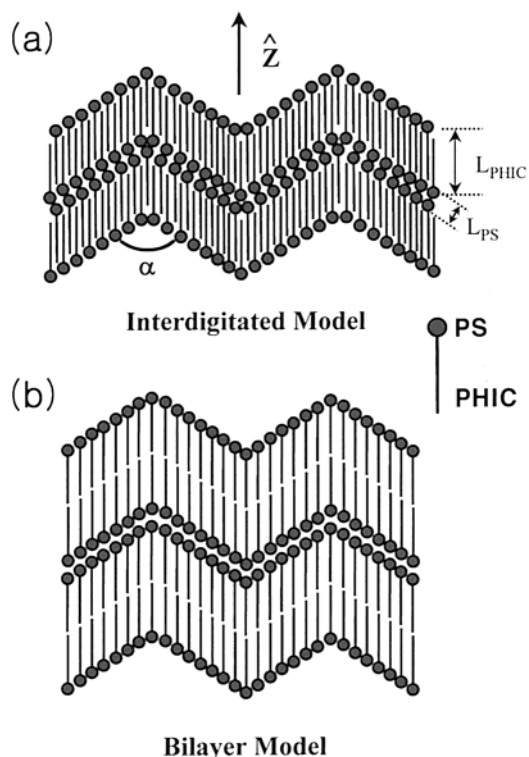


Figure 5. Schematic representation of (a) interdigitated model and (b) bilayer model in the zigzag morphology.

the interdigitated model was suggested to be more consistent with domain spacing predictions based on molecular weight data.

With additional research into the influence of the rod volume fraction on the phase behavior, the authors studied the rod–coil copolymers with varying compositions of rod blocks.⁵² Transmission electron microscopy revealed phase-separated morphologies with rod-rich regions and coil-rich regions in which rod segments are organized into tilted layers analogous to those observed in smectic phases. In these layers, the polymer backbone axis is tilted at an angle relative to the layer normal. It was suggested that the tilting of rod segments might produce a greater volume for coil segments to explore conformational space. This would be particularly important as the molar mass of the coil segment increases due to the proportional increase in the average equilibrium

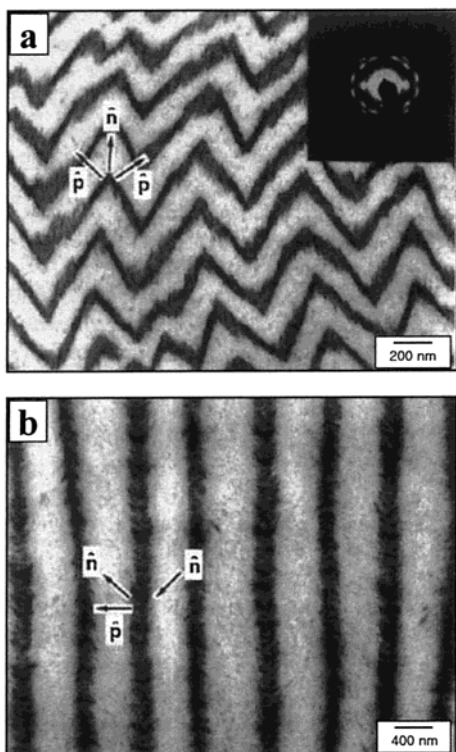


Figure 6. TEM images for (a) zigzag lamellar morphology of rod-coil copolymer with $f_{\text{rod}} = 0.90$ and (b) arrowhead morphology of rod-coil copolymer with $f_{\text{rod}} = 0.98$. (Reprinted with permission from ref 52. Copyright 1996 American Association for the Advancement of Science).

cross section with respect to the degree of polymerization. A rod-coil copolymer with a rod volume fraction $f_{\text{rod}} = 0.42$ organizes into a wavy lamellar morphology, in which the rod blocks are tilted with respect to the lamellar normal by approximately 60° . Small-angle electron diffraction patterns revealed that the rod domains are crystalline and that the local orientation of the stiff rod blocks extends up to $1 \mu\text{m}$.

Rod-coil copolymers with rod volume fractions $f_{\text{rod}} = 0.73$ and $f_{\text{rod}} = 0.90$ were observed to form a zigzag morphology consisting of alternating rod and coil layers arranged in a zigzag fashion. The rod axis is tilted with respect to the layer normal by approximately 45° , and the rod blocks are crystalline as confirmed by the small-angle electron diffraction. The formation of two distinct sets of lamellar with equal that opposite orientations from the local rod directors was suggested to be a consequence of the nucleation of the smectic C phase in a thin film. The rod-coil copolymers with a short polystyrene coil and a very long rod block ($f_{\text{rod}} = 0.96$ and $f_{\text{rod}} = 0.98$) form an interesting different morphology as evidenced by transmission electron microscopy. The authors described this morphology as the *arrowhead* morphology because tilted layers in a chevron pattern are spaced by arrowhead shaped domains of polystyrene which alternatively flip by 180° . Presumably, the alternating direction of the arrowheads reflects the deformation experienced by polystyrene coils as the layer normal in adjacent layers alternate between 45° and -45° . In terms of rod packing with the rod

domains, a bilayer and an interdigitated model were suggested to be most consistent for the polymers with $f_{\text{rod}} = 0.96$ and $f_{\text{rod}} = 0.98$. A series of morphologies including zigzag lamellar to arrowhead microdomain structures observed by transmission electron microscopy is shown in Figure 6 and the structural packing model is shown in Figure 7. A preliminary morphol-

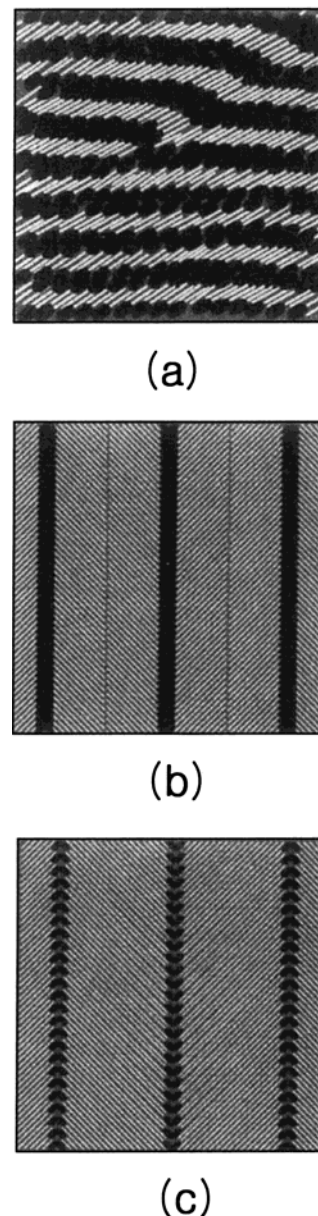


Figure 7. Structural packing models for (a) wavy lamellar, (b) bilayer arrowhead, and (c) interdigitated arrowhead morphologies in rod-coil copolymers **2**. (Reprinted with permission from ref 52. Copyright 1996 American Association for the Advancement of Science).

ogy diagram for this rod-coil system was suggested as shown in Figure 8, based on these experimental results.⁵³ As solvent is evaporated, the rod-coil solutions are predicted to form a homogeneous lyotropic nematic liquid crystal phase prior to microphase separation which supports rod-coil theories.^{12,36–38} Further evaporation of solvent causes microphase separation into various lamellar structures depending on the rod volume fraction of the molecule.

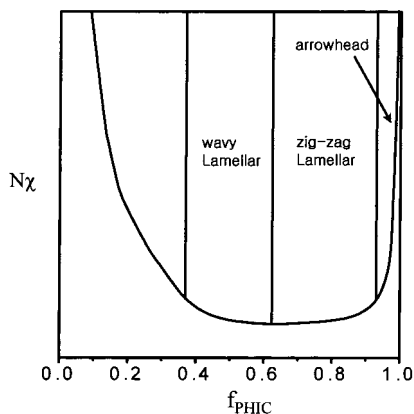
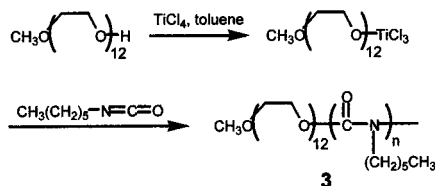


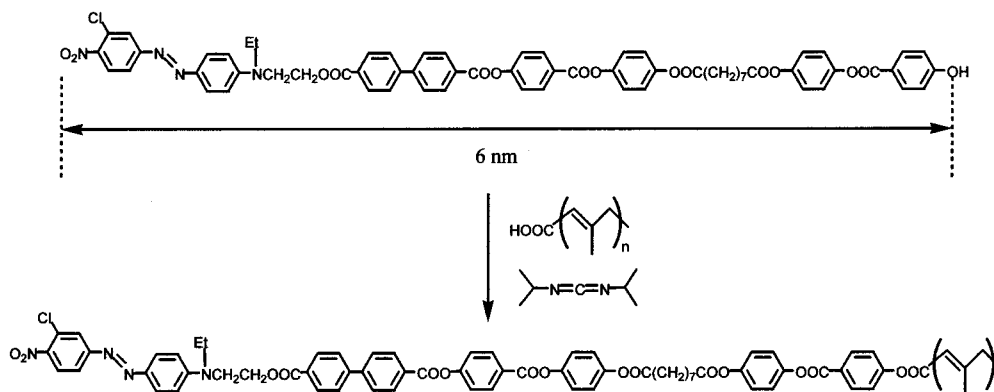
Figure 8. Morphology diagram for rod-coil diblock copolymers (**2**).

Scheme 3



Recently, Pearce et al. reported on rod-coil copolymers consisting of poly(hexyl isocyanate) as the rod block and poly(ethylene oxide) as the coil block (Scheme 3).⁵⁴ The copolymers (**3**) were obtained by coordination polymerization of *n*-hexyl isocyanate initiated by TiCl_3 end functionalized poly(ethylene oxide). A block copolymer with poly(ethylene oxide) with 12 repeating units and poly(hexyl isocyanate) with 50 repeating units exhibits lyotropic liquid crystalline phases in concentrated toluene solution (above 20 wt %) as determined by optical polarized microscopy. When the block copolymer film was cast from the dilute toluene solution, a nematic-like domain texture was observed. However, when cast from a mixture of toluene and pentafluorophenol, where the poly(hexyl isocyanate) block is converted from rod to coil configuration, the liquid crystalline phase behavior disappears. The tendency of the rod segments to be arranged into anisotropic order along their axes seems to play an important role in liquid crystalline behavior of the polymer.

Scheme 4



IV. Rod–Coil Copolymers Based on Mesogenic Rods

A. Bulk-State Supramolecular Structures

It is well-known that classical rodlike mesogenic molecules arrange themselves with their long axes parallel to each other to give rise to nematic and/or layered smectic types of supramolecular structures.^{6,7} Because of the preferred parallel arrangement of the rigid, rodlike units, the formation of curved interfaces is strongly hindered in the mesogenic rods. On the contrary, rod-coil block systems based on mesogenic rods can provide a variety of supramolecular structures due to the effect of microphase separation and the molecular anisometry of rod block. Even though the molecular weight is very small, microphase separated structures can form due to large chemical differences between each block. In addition to various layered structures as described in Ober's rod-coil copolymers,^{51,52} the stiff rod blocks might assemble into finite nanostructures at higher coil volume fractions as predicted by rod-coil theories.^{15,36–38}

Stupp et al. reported on rod-coil copolymers consisting of an elongated mesogenic rod and a monodisperse polyisoprene (Scheme 4).^{55–57} The living polyisoprene was converted to a carboxylic acid group with CO_2 , and the rod having a well-defined structure with a fully extended rod length of 6 nm was synthesized by conventional synthetic methods. The final rod-coil polymers (**4**) with the rod volume fractions range from 0.19 to 0.36 were prepared by esterification of an acid functionalized polyisoprene and a hydroxy functionalized rod block in the presence of diisopropylcarbodiimide (DIPC).

These rod-coil copolymers organize into ordered structures that differ in terms of varying the rod volume fraction as monitored by transmission electron microscopy and electron tomography. The rod-coil copolymer with rod volume fraction $f_{\text{rod}} = 0.36$ forms alternating rod- and coil-rich strips 6–7 and 5–6 nm wide, respectively. Electron tomography revealed that the copolymers self-assemble into layered 2-D superlattices and ordered 3-D morphology. Slices orthogonal to the plane of the film showed that the rod-domains are not lamellae but discrete channel-like long objects, 6–7 nm in diameter. In strip

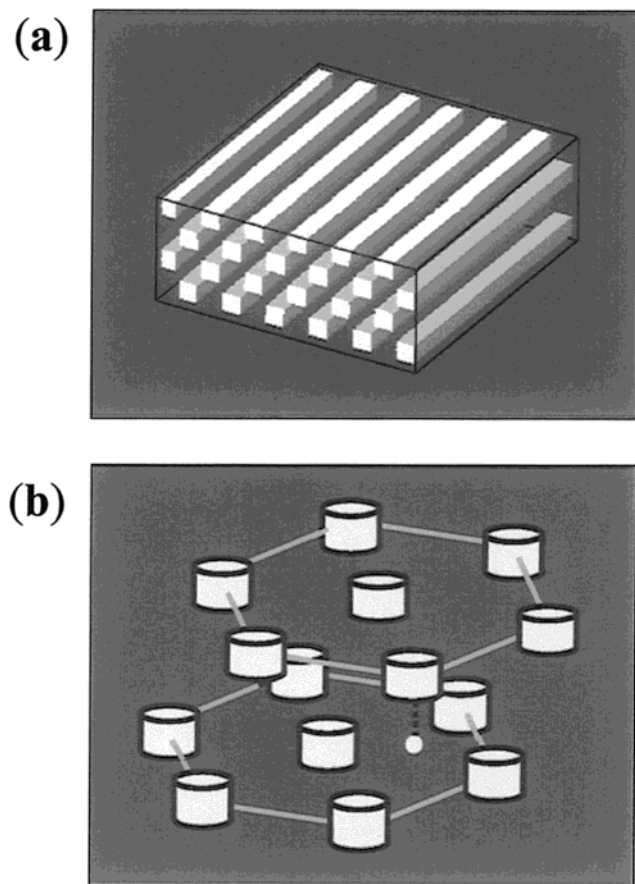
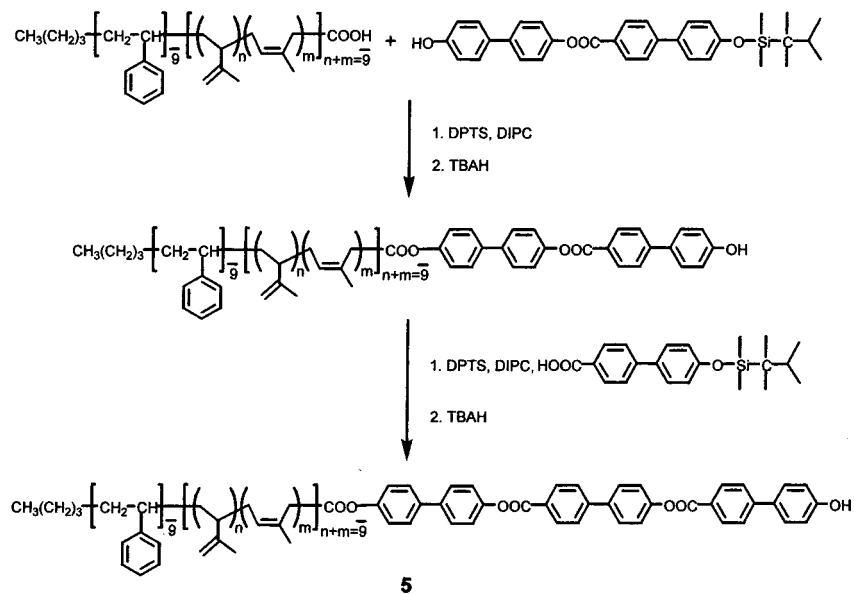


Figure 9. Schematic diagrams of (a) strip morphology of rod-coil copolymer with $f_{\text{rod}} = 0.36$ and (b) hexagonal superlattice of rod-coil copolymer with $f_{\text{rod}} = 0.25$. (Reprinted with permission from ref 57. Copyright 1997 American Chemical Society).

morphology, layers are correlated such that each strip resides over a coil region of the adjacent layer and that the direction of its long axis remains constant through the layers as illustrated in Figure 9a. The rod segments are thought to assemble into interdigitated bilayer or monolayer.

Scheme 5



The rod-coil copolymer with $f_{\text{rod}} = 0.25$ forms a hexagonal superlattice of rod aggregates measuring approximately 7 nm in diameter and a domain spacing of 15 nm as evidenced by transmission electron micrograph. By studying the films by electron tomography, the authors observed that each layer contains a hexagonal superlattice. Slices orthogonal to the film plane showed that the rod aggregates are discrete objects with roughly the same dimensions in all directions as schematically illustrated in Figure 9b. The rod-coil copolymer with $f_{\text{rod}} = 0.19$ does not show phase separated morphology in the as-cast state. Interestingly, annealing the film near 100 °C produced a hexagonal superlattice with long-range order comparable to $f_{\text{rod}} = 0.25$. These works clearly show that the supramolecular structure formed by self-assembly of rod segments can be controlled by simple variation of rod to coil volume ratio.

The authors also synthesized triblock rod-coil copolymers containing oligostyrene-*block*-oligoisoprene as the coil block and three biphenyl units connected by ester linkages as the rod block (Scheme 5).^{58,59} Carboxylic acid functionalized coil block was prepared by anionic sequential living polymerization of styrene and then isoprene, followed by end capping with CO₂. The resulting coil block was then connected to a rigid block made up of two biphenyl units through an ester bond, followed by deprotection at the phenolic terminus. The final rod-coil copolymers were synthesized by following the same sequence of reactions, i.e., esterification and then subsequent deprotection of a protecting silyl group.

The rod-coil copolymer containing a (styrene)₉-(isoprene)₉ block oligomer (5) as coil segment was observed to self-assemble into uniform narrow-sized aggregates and to subsequently organize into a superlattice with periodicities of 70 and 66 Å as evidenced by transmission electron microscopy (Figure 10a) and small-angle electron diffraction.⁵⁸ The wide-angle electron diffraction pattern revealed an a^*b^* reciprocal lattice plane, suggesting that the rod

Chart 1

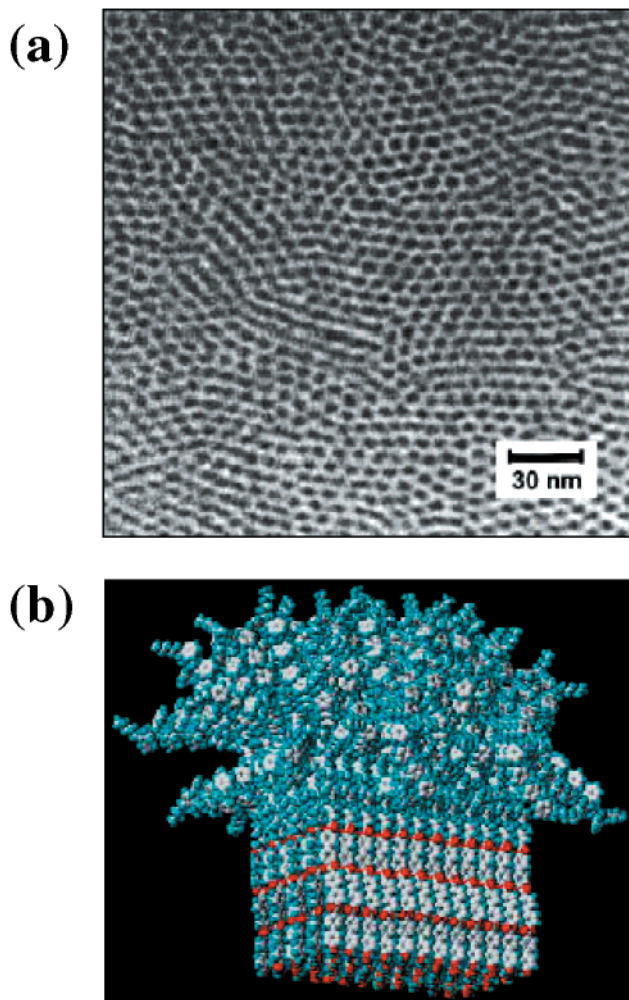
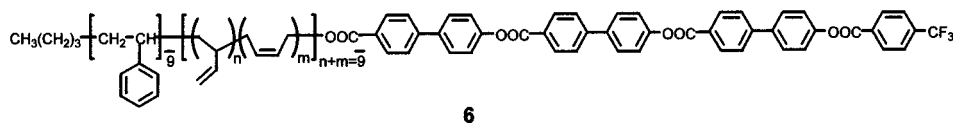


Figure 10. (a) TEM image (Reprinted with permission from ref 59. Copyright 2000 American Chemical Society) and (b) schematic packing structure of rod–coil copolymer (5) (Reprinted with permission from ref 58. Copyright 1997 American Association for the Advancement of Science).

segments are aligned axially with their preferred direction with respect to the plane normal of the layer with long-range order. Transmission electron microscopy of the microtomed sections revealed a layered structure with characteristic periods of the 70 Å layers consisting of one dark and one light band with thicknesses of 30 and 40 Å, respectively. On the basis of these experimental data together with molecular modeling calculations, the authors proposed that these rod–coil copolymers self-assemble into fascinating mushroom-shaped supramolecular structures containing 100 rod–coil molecules with a molar mass about 200 kD, which assemble in a “cap to stem” arrangement (Figure 10b). Spontaneous polar organization in this system was reported and was presumably due to the nature of the supramolecular units of molecule preformed in solution. Both microphase separation between the two coil blocks and the crystallization of the rod segments are likely to

play important roles in the formation of the unusual mushroom-shaped aggregate. This leads to the asymmetrical packing of the nanostructures that form micrometer-sized platelike objects exhibiting tape-like characteristics with nonadhesive-hydrophobic and hydrophilic-sticky opposite surfaces.

Molecular object polymers have distinct and permanent shapes similar to proteins with a well-defined folded shape. Stupp et al. presented an elegant approach to produce well-defined macromolecular objects converting supramolecular clusters by polymerization of cross-linkable group within a discrete supramolecular unit.⁶⁰ The rod–coil triblock molecule (6) synthesized by the authors is composed of a block of oligostyrene, a block of polymerizable oligobutadiene, and a rodlike block containing CF₃ end group which has a large dipole moment (Chart 1).

Transmission electron microscopy revealed that the triblock molecules self-assemble into a solid-state structure consisting of aggregates ~2 nm in diameter. The thickness of layers revealed by small-angle X-ray scattering appears to be 8 nm. The rod axes in the cluster were observed to be normal to the layers and be perpendicular to the plane of the TEM micrographs as confirmed by wide-angle electron diffraction patterns. On the basis of these data, the rod–coil triblock molecules were suggested to pack into the mushroom-shaped nanostructure with a height of 8 nm and a diameter of 2 nm. Each supramolecular nanostructure was estimated to contain approximately 23 molecules. Most important, this nanostructure was proposed to impart the spatial isolation of cross-linkable oligobutadiene blocks required to form a well-defined object. Therefore, polymerization might be confined to the volume of the supramolecular cluster. Thermal polymerization of rod–coil triblock molecules in liquid crystalline state produced high molar-mass products with a very narrow polydispersity within a range from 1.15 to 1.25 and molecular weight of approximately 70 000 as confirmed by GPC (Figure 11). The macromolecular objects obtained reveal an anisotropic shape (2 by 8 nm) similar to that of supramolecular clusters, as determined by electron microscopy and small-angle X-ray scattering. Polarized optical microscopy showed that polymerization of the triblock molecules into macromolecular objects results in a strong stabilization of the ordered structure that remains up to a chemical decomposition temperature of 430 °C. This result is interesting because the self-assembly process provides a direct pathway to prepare well-defined molecular nano-objects with distinct and permanent shape through polymerization within supramolecular structures.

A strategy to manipulate the nanostructure assembled by rod building blocks may be accessible by attaching a bulky dendritic wedge to a rod end. As the cross-sectional area of rod segment increases

Chart 2

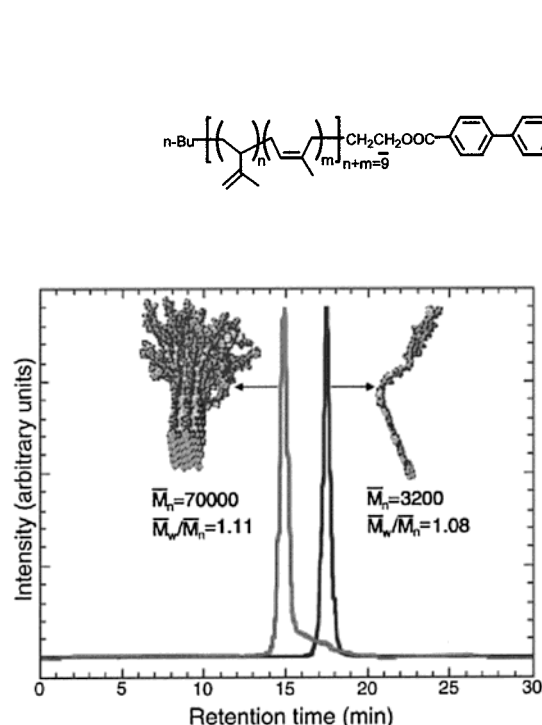


Figure 11. GPC traces of rod-coil triblock molecule (**6**) and macromolecular object. (Reprinted with permission from ref 60. Copyright 1999 American Association for the Advancement of Science).

while maintaining anisotropic order of rod segments, greater steric repulsion between rod segments could possibly frustrate the formation of two-dimensional assemblies. An interesting example of dendron rod-coil molecules synthesized recently by Stupp and co-workers is depicted in Chart 2.⁶¹

In contrast to previously described structurally simple rod-coil molecules, these dendron rod-coil molecules (**7**) form well-defined ribbonlike 1-D nano-

structure. When cast from a 0.004 wt % solution of the CH_2Cl_2 solution onto a carbon support film, one-dimensional objects with a uniform width of 10 nm were observed by the transmission electron microscopy (TEM), in which the objects build networks that cause the dilute CH_2Cl_2 solution (as low as 0.2 wt %) to undergo gelation (Figure 12a). Atomic force microscopy (AFM) revealed their thickness of 2 nm, indicative of a ribbonlike shape. The crystal structure of the model compound made up of a dendron identical to that presented in **7** but covalently attached to only one biphenyl revealed 8 hydrogen bonds that connect the tetramers along the axis of the ribbon. The thickness of the tetrameric cycles was measured to be 2 nm, which is in good agreement with the thickness of the nanoribbons as determined by AFM. On the basis of these results as well as the crystal structure of the model compound, the supramolecular structure was proposed to be a ribbonlike structure with a width of 10 nm and a thickness of 2 nm (Figure 12b). π - π stacking interactions between aromatic segments and directional hydrogen bonding seem to play important roles in the formation of this well-defined novel nanostructure.

Lee et al. also reported on small rod-coil systems with a mesogenic rod segment. Their molecules are based on flexible poly(ethylene oxide) or poly(propylene oxide) as a coil block.^{62,63} The rod-coil molecule based on poly(ethylene oxide) coil (**8**) exhibits a

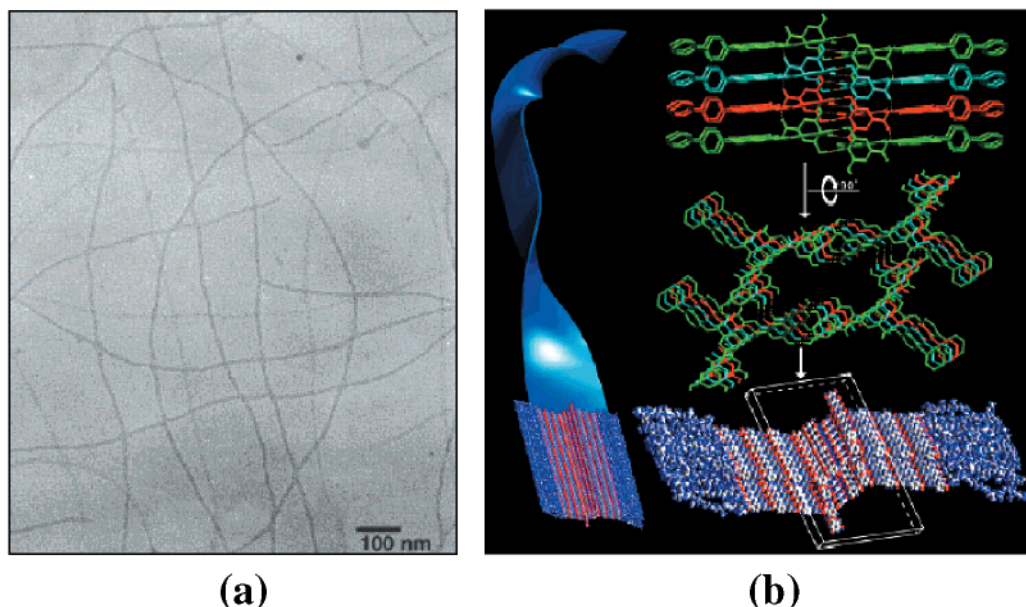
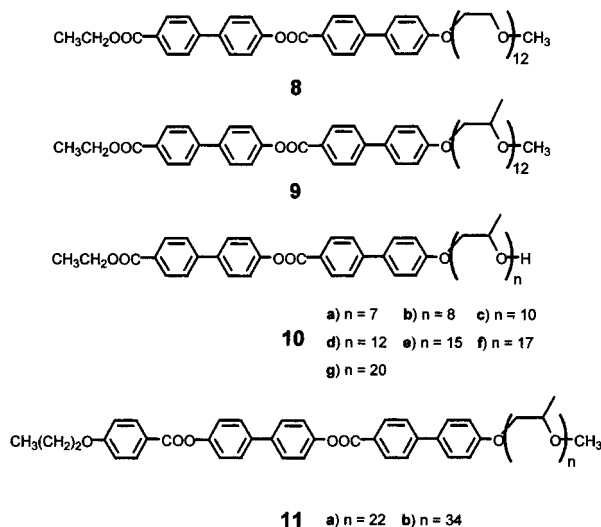


Figure 12. (a) TEM image of nanoribbons formed in dichloromethane. (b) Schematic representation of supramolecular nanoribbon by self-assembly of dendron rod-coil molecules. (Reprinted with permission from ref 61. Copyright 2001 American Chemical Society).

smectic A phase, whereas the latter molecule (**9**) shows a hexagonal columnar structure.⁶³ This large structural variation between the molecularly similar systems should be caused by the larger spatial requirement of the bulkier poly(propylene oxide) coil in comparison with the poly(ethylene oxide).

In a more systematic work on the influence of the coil length on phase behavior, the authors studied rod–coil molecules (**10**) with poly(propylene oxide) having different degrees of polymerization but the identical rod segment (Chart 3).^{64,65} A dramatic

Chart 3



structural change in the melt state of this rod–coil system was observed with variation in the coil length as determined by a combination of techniques consisting of differential scanning calorimetry (DSC), optical polarized microscopy, and X-ray scattering. Rod–coil molecules with 7 and 8 propylene oxide units exhibit layered smectic C and smectic A phases, while rod–coil molecules with 10 to 15 repeating units exhibit an optically isotropic cubic phase. This structure was identified by the X-ray scattering method to be a bicontinuous cubic phase with $Ia3d$ symmetry. Further increasing the coil length induces a hexagonal columnar mesophase as in the case of the molecules with 15 to 20 repeating units (Figure 13). Organization of the rod–coil molecules into a cross sectional slice of a cylinder for cubic and columnar phases is thought to give rise to a aromatic core with approximately square cross section taking into account the calculation based on the lattice parameters and densities. The sizes and periods of these supramolecular structures are typically in a range of less than 10 nm.

Supramolecular structures of rod–coil diblock molecules consisting of more elongated rod segment and PPO coil segment (**11**) were also investigated by the authors (Chart 3).⁶⁶ In these rod–coil molecules, the rod segment consists of two biphenyl and a phenyl group connected through ester linkages. Thus, the tendency of this system to self-organize into layered structures at a given rod volume fraction was expected to be stronger than that of the rod–coil system containing only two biphenyl units as the rod block. These rod–coil molecules with 22 (**11a**) and 34 (**11b**)

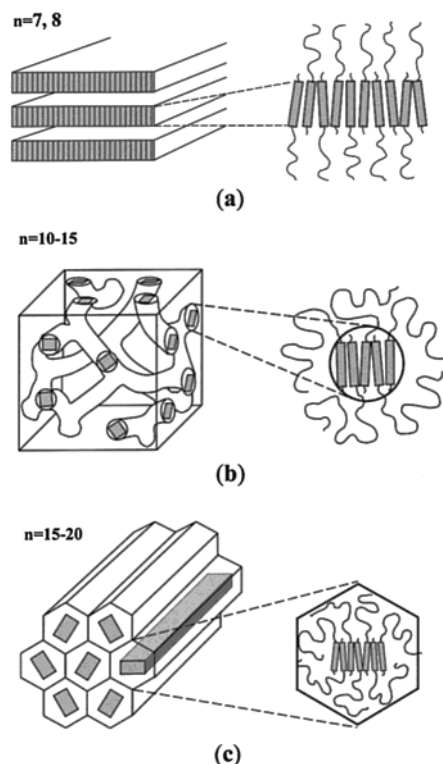


Figure 13. Schematic representation of supramolecular structures of rod-coil molecules **10**. (a) Smectic A, (b) bicontinuous cubic, and (c) hexagonal columnar phases. (Reprinted with permission from ref 64. Copyright 1998 American Chemical Society).

PPO repeating units self-assemble into a supramolecular honeycomb-like layered structure, in which perforations are filled by coil segments. When cast from dilute CHCl_3 solution onto a carbon support film, honeycomb-like supramolecular structure was observed, as revealed by transmission electron microscopy (TEM), in which coil perforations are packed on a hexagonal symmetry with distances between perforations of approximately 10 nm (Figure 14a).

Electron diffraction patterns revealed very well-oriented, single crystal-like reflections associated with the a^*b^* reciprocal plane of a rectangular lattice, indicating that the rod segments are aligned axially with their preferred direction with respect to the plane normal of the layer. Small-angle X-ray diffraction pattern showed a number of sharp reflections that are indexed as a 3-dimensional hexagonal structure (Figure 14b). On the basis of these results as well as density measurements, the supramolecular structure was proposed to be a honeycomb-like crystalline layer of the rod segments with in-plane hexagonal packing of coil perforation as illustrated in Figure 15. The consequent layers were suggested to be stacked in ABAB arrangement to generate 3-dimensional order. The diameters of perforation sizes were estimated to be approximately 6.5 nm as confirmed by TEM, SAXS, and density measurements. These dimensions are comparable to those to Bacillaceae in which pores with regular size are organized predominantly into a hexagonal lattice. Thus, this system might provide access to an excellent model for exploring biological processes in supramolecular materials.

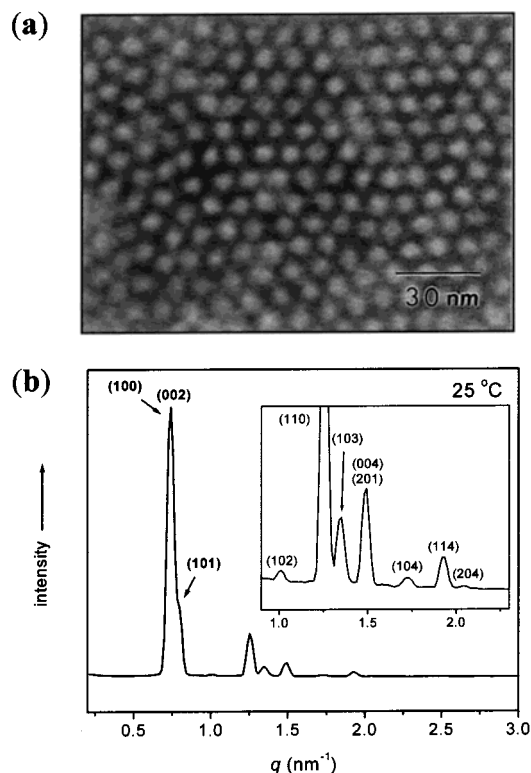
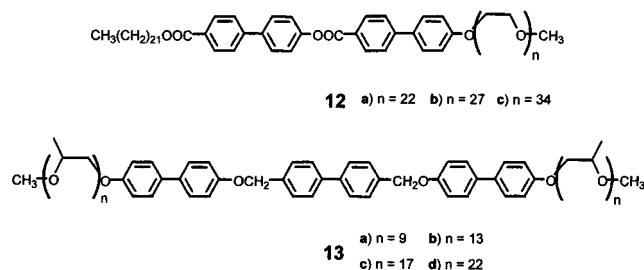


Figure 14. (a) TEM image and (b) small-angle X-ray diffraction pattern of rod-coil molecule **11b**. (Reprinted with permission from ref 65. Copyright 2001 American Chemical Society).

Lee et al. also reported the assembling behavior of coil-rod-coil ABC triblock molecules where the rod block is connected as the middle block, consisting of poly(ethylene oxide) with different degrees of polymerization, two biphenyl unit as rod and docosyl coil (Chart 4).⁶⁷ All of the coil-rod-coil ABC triblock molecules (**12**) exhibit three different crystalline melting transitions associated with poly(ethylene oxide), docosyl, and rod blocks, respectively, as determined by DSC, indicative of phase separation among blocks.

Interestingly, molecules with 22 to 34 ethylene oxide repeating units exhibit a hexagonal columnar

Chart 4



mesophase which, in turn, undergoes transformation into discrete spherical micellar structure with a lack of symmetry (Figure 16). Small-angle X-ray diffraction in the optically isotropic state revealed a strong primary peak together with a broad peak of weak intensity at about 1.8 relative to the primary peak position, indicating that the spatial distribution of centers of the spherical micelles has only liquidlike short range order, most probably due to random thermal motion of spherical micelles. From the observed primary peak of X-ray diffraction, the diameter (d) of spheres was estimated to be approximately 13 nm. It is likely that hydrophobic force plays an important role in the self-assembly of the molecules into discrete nanostructures.

In a separated work, the authors reported on supramolecular structural behavior of symmetric coil-rod-coil molecules (**13**) consisting of three biphenyl units with ether linkages as the rod segment and poly(propylene oxide) with different degrees of polymerization (Chart 4).⁶⁸ Molecules with a certain length of coil (DP of PPO = 9 to 22) assemble into discrete supramolecular aggregates that spontaneously organize into a novel 3-D tetragonal phase with a body-centered symmetry in the solid and melt states as determined by small-angle X-ray scattering (Figure 17).

On the basis of X-ray data and density measurements, the authors proposed that the inner core of the supramolecular aggregate is constituted by the discrete rod bundle with a cylindrical shape with 5 nm in diameter and 3 nm in length that is encapsu-

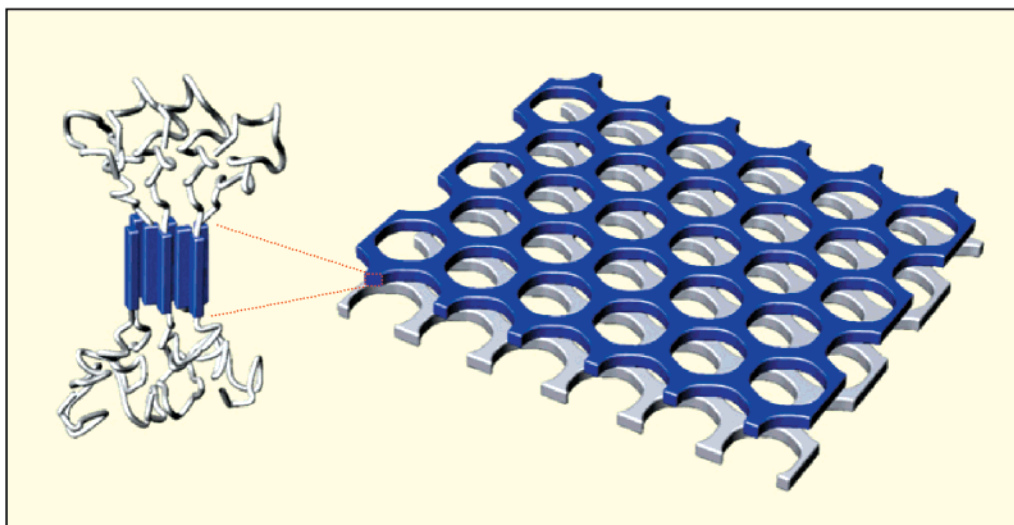


Figure 15. Schematic diagram for the honeycomb-like layer formed by the rod segments of rod-coil molecule **11b**. (Reprinted with permission from ref 65. Copyright 2001 American Chemical Society).

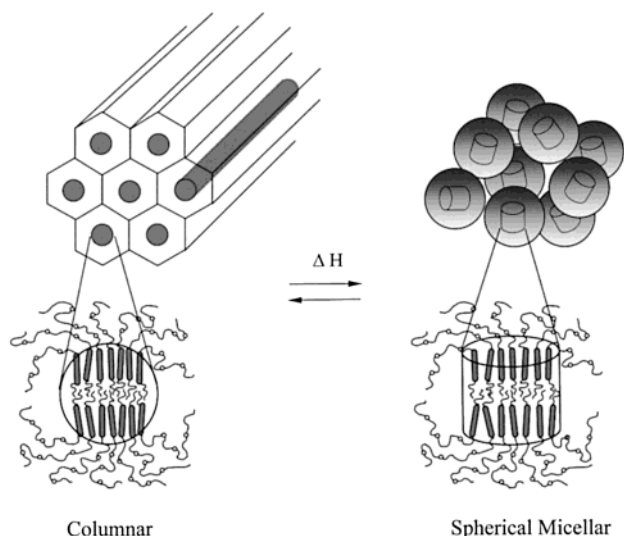


Figure 16. Schematic representation for the organization of the hexagonal columnar and spherical micellar phases of rod-coil molecules **12a–c**. (Reprinted with permission from ref 66. Copyright 1998 American Chemical Society).

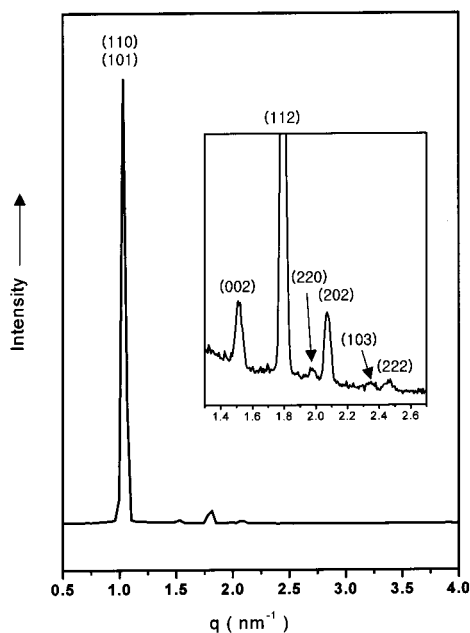


Figure 17. Small-angle X-ray scattering pattern of rod-coil molecule **13c**. (Reprinted with permission from ref 67. Copyright 2000 American Chemical Society).

lated with phase-separated poly(propylene oxide) coils, which gives rise to the formation of nonspherical oblate aggregate as illustrated schematically in Figure 18. The supramolecular rod bundles subse-

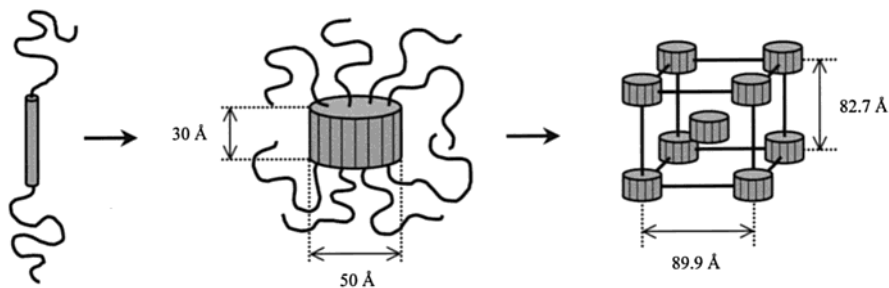
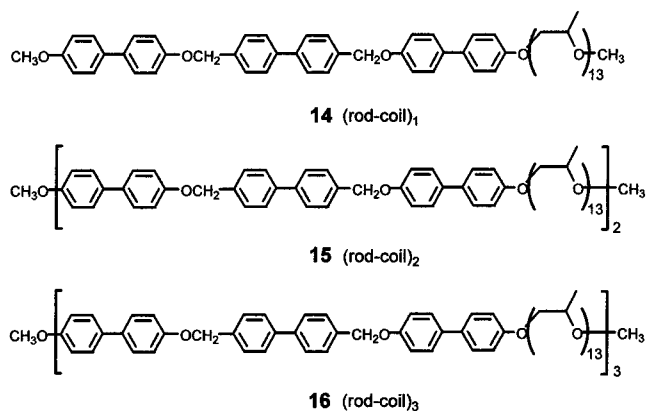


Figure 18. Schematic diagram of self-assembly of **13c** into a supramolecular bundle and the subsequent formation of the body-centered tetragonal lattice. (Reprinted with permission from ref 67. Copyright 2000 American Chemical Society).

Chart 5



quently organize into a 3-D body-centered tetragonal symmetry. The oblate shape of supramolecular aggregates is believed to be responsible for the formation of unusual 3-D tetragonal phase. The authors suggested that this unique phase behavior is mostly originated from the anisotropic aggregation of rod segments with their long axes within microphase separated aromatic domains. Consequently, rod bundles with a puck-like cylindrical shape would give rise to oblate micelles that can pack more densely into an optically anisotropic 3-dimensional tetragonal lattice, rather than an optically isotropic cubic lattice.

The rod-coil approach as a means to manipulate supramolecular structure as a function of rod volume fraction was reported to be extended to main chain multiblock copolymer systems.⁶⁹ In contrast to this, another strategy to manipulate the supramolecular structure at constant rod-to-coil volume ratio can also be accessible by varying the number of grafting sites per rod which might be closely related to the grafting density at the interface separating rod and coil segments.⁷⁰ For this reason, Lee et al. synthesized (rod-coil)₁ (**14**), (rod-coil)₂ (**15**), and (rod-coil)₃ (**16**) with rod-coil repeating units consisting of three biphenyl units connected by methylene ether linkages as the rod block and poly(propylene oxide) with DP of 13 as the coil block (Chart 5).

All of the oligomers are self-organized into ordered supramolecular structures that differ significantly on variation of the number of repeating units as confirmed by X-ray scattering. The (rod-coil)₁ shows a lamellar crystalline and a bicontinuous cubic liquid crystalline structures. In contrast, the (rod-coil)₂ shows a 2-D rectangular crystalline and a tetragonal columnar liquid crystalline structure, while the (rod-coil)₃ displays a hexagonal columnar structure in both

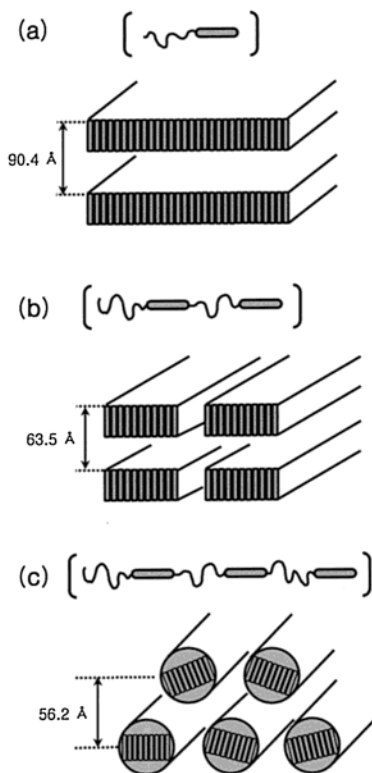


Figure 19. Schematic representation for the formation of (a) lamellar of the (rod-coil)₁, (b) 2-D rectangular of the (rod-coil)₂, and (c) hexagonal columnar of the (rod-coil)₃. (Reprinted with permission from ref 70. Copyright 2001 American Chemical Society).

their solid and melt states (Figure 19). These results represent that self-assembled solid state structure, from 1-D lamellar, 2-D rectangular to 2-D hexagonal lattices are formed by rod-coil structures that differ only in the number of repeating units. This interesting variation of self-assembled structures, at an identical rod to coil volume ratio, was explained by considering the density of grafting sites at the interface separated by rod and coil segments as shown in Figure 20.

B. Supramolecular Structures from Binary Mixtures

Rod-coil copolymers are a type of amphiphile that can self-assemble into a variety of ordered nanostructures in a selective solvent.^{36,37,71} In solvents that selectively dissolve only coil blocks, rod-coil copolymers can form well-defined nanostructures with rod domain consisting of the insoluble block. This results in an increase of the relative volume fraction of the coil segments relative to the rod segments, which gives rise to various supramolecular structures. Particularly, poly(alkylene oxide) as the coil block of rod-coil molecule has additional advantages due to complexation capability with alkali metal cation, which can provide an application potential for solid polyelectrolytes and induce various supramolecular structures.^{72–75}

Lee et al. showed that control of the supramolecular structure in rod-coil molecular systems containing either poly(ethylene oxide) (**8**) or poly(propylene oxide) (**17**) coils and induction of ordered structures

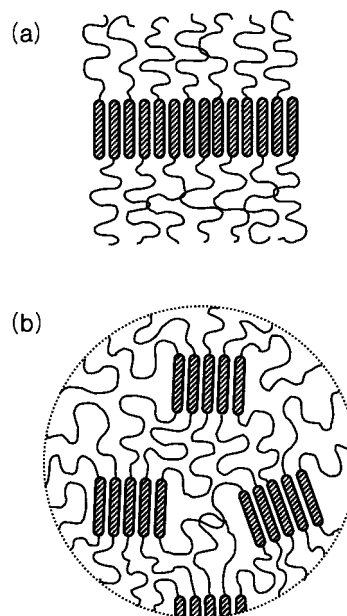
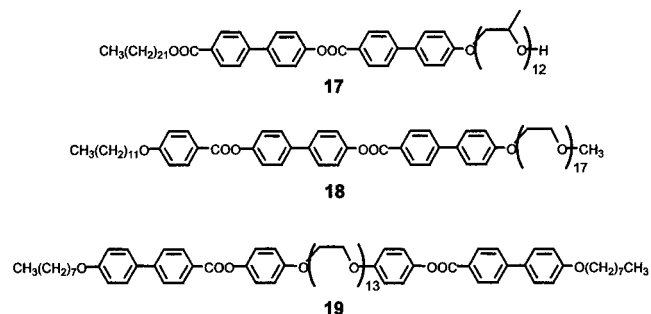


Figure 20. Schematic representation of the molecular arrangement of rod-coil units in (a) (rod-coil)₁ and (b) rod-coil multiblock copolymer. (Reprinted with permission from ref 70. Copyright 2001 American Chemical Society).

Chart 6



are possible through complexation with lithium ion (Chart 6).^{76–79}

First of all, the authors investigated the influence of complexation with LiCF₃SO₃ on the phase behavior of rod-coil diblock molecule containing poly(ethylene oxide) with DP of 12 as the coil block (**8**).⁷⁷ The complexes with 0.0–0.15 mol of LiCF₃SO₃/ethylene oxide unit ([Li⁺]/[EO]) were observed to exhibit only a smectic A mesophase, while the complex with [Li⁺]/[EO] = 0.20 shows an optical isotropic cubic phase in addition to a high-temperature smectic A phase. The complex with [Li⁺]/[EO] = 0.25 exhibits only a bicontinuous cubic phase, and the smectic A phase is suppressed for this complex. On melting of complexes with [Li⁺]/[EO] = 0.30 and 0.35, a cubic phase is also formed; however, further heating gives rise to a 2-D hexagonal columnar mesophase as evidenced by X-ray scattering. Complexes with [Li⁺]/[EO] = 0.40–0.70 exhibit only a columnar phase. As shown in the binary phase diagram of Figure 21, the supramolecular structure in the melt state of the rod-coil molecule changes successively from smectic A through bicontinuous cubic to hexagonal columnar structures as the salt concentration increases.

Complexation of rod-coil molecules with LiCF₃SO₃ also induces an ordered supramolecular structure.⁷⁸

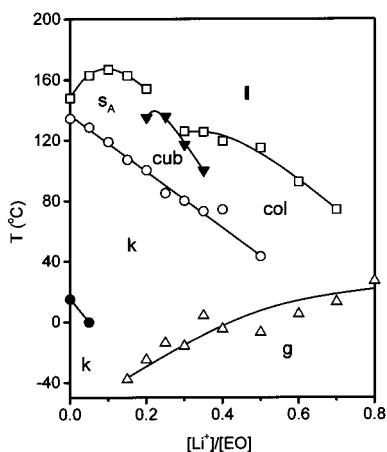


Figure 21. Phase diagram of the complexes of **8** with lithium triflate (g = glassy, k = crystalline, s_A = smectic A, cub = cubic, col = columnar, i = isotropic).

The coil-rod-coil triblock molecule (**17**) based on poly(propylene oxide) (PPO) coil segment was observed to show only an isotropic liquid upon melting. In contrast, the addition of greater than 0.10 mol of lithium salt/propylene oxide (PO) unit induces the formation of a liquid crystalline order (Figure 22).

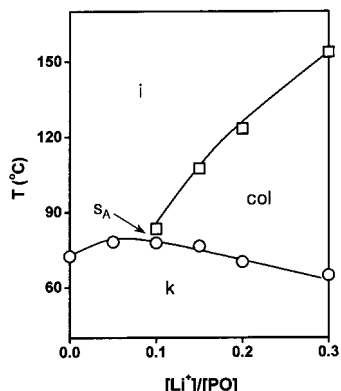


Figure 22. Phase diagram of the complexes of **17** with lithium triflate (k = crystalline, s_A = smectic A, col = hexagonal columnar, i = isotropic).

The complex with $[Li^+]/[PO] = 0.10$ exhibits a crystalline melting transition followed by a smectic A mesophase. By increasing the salt concentration as in the case of complexes with $[Li^+]/[PO] = 0.15 \sim 0.30$, the smectic A phase is suppressed; instead, they exhibit a hexagonal columnar mesophase as evidenced by X-ray scattering. The induction of ordered structure in the melt state of the rod-coil molecule by complexation is most probably due to enhanced microphase separation between hydrophobic blocks and poly(propylene oxide) block caused by transformation from a dipolar medium to an ionic medium in poly(propylene oxide) coil.

Rod-coil molecular architecture containing poly(ethylene oxide) endows an amphiphilic character as discussed earlier, and thus hydrophilic solvents such as acryl amide would be selectively dissolved in the microphase-separated coil domains, which gives rise to a variety of supramolecular structures. Polymerization of acryl amide solution in ordered state can give rise to ordered nanocomposite materials. Similar

to rod-coil complexes with $LiCF_3SO_3$,⁷⁷ the acryl amide solution of a rod-coil molecule (**18**) was reported to show a phase transition from layered smectic to columnar phase with a bicontinuous cubic phase as the intermediate regime with increasing acryl amide content (Figure 23).⁸⁰ More importantly,

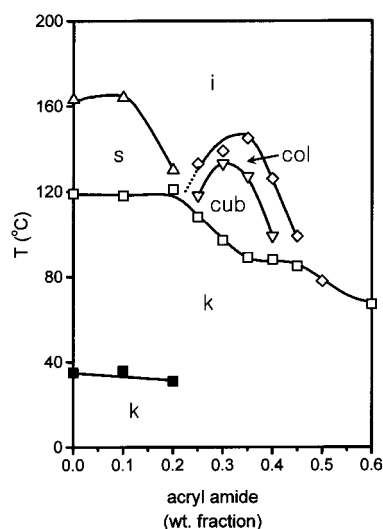


Figure 23. Phase diagram of **18** with acryl amide (k = crystalline, s = smectic, cub = bicontinuous cubic, col = hexagonal columnar, i = isotropic).

this organized polymerizable solution can be used for construction of ordered aromatic-aliphatic nanocomposite materials. Thermal polymerization of the hexagonally ordered solution containing acryl amide and 0.5 mol % of 2,2'-azobisisobutyronitrile with respect to acryl amide at 130 °C for 24 h was observed to produce a hexagonally ordered nanocomposite material with a primary spacing of 4.8 nm as monitored by FT-IR and small-angle X-ray scattering. As illustrated in Figure 24, the acryl amide would be selectively dissolved by hydrophilic PEO coil

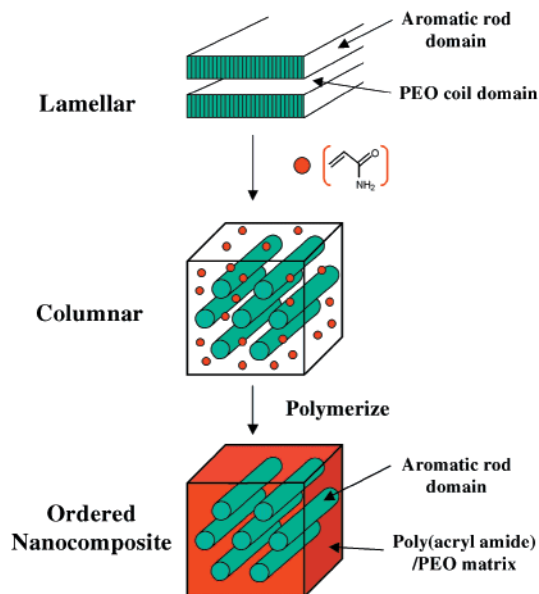


Figure 24. Schematic diagram for the induction of a hexagonal columnar structure by addition of acryl amide and subsequent formation of ordered nanocomposite through polymerization.

domains in a lamellar structure, creating a spontaneous interfacial curvature between the rod and PEO/acryl amide which induces a hexagonal columnar structure. Upon polymerization, the system retains the hexagonally ordered nanostructure consisting of aromatic rod domains in a poly(acryl amide)/PEO matrix to construct ordered aromatic–aliphatic nanocomposite.

Kato et al. reported on rod–coil–rod molecules consisting of rigid mesogenic cores and flexible poly(ethylene oxide) coils.⁸¹ The small triblock molecule (**19**) (Chart 6) was observed to exhibit smectic A liquid crystalline phase as determined by a combination of optical polarized microscopy and differential scanning calorimetry. The incorporation of LiCF_3SO_3 into the rod–coil–rod molecules shows significant mesophase stabilization. X-ray diffraction patterns revealed that complexation of **19** ($[\text{Li}^+]/[\text{EO}] = 0.05$) drastically reduces the layer spacing from 44 to 23 Å. This decrease is thought to be due to the interaction of the lithium salt with the ether oxygen which results in a more coiled conformation of the poly(ethylene oxide) coil. Ion conductivities were also measured for complexes forming homeotropically aligned molecular orientation of the smectic phase. Interestingly, the highest conductivity was observed for the direction parallel to the layer (Figure 25).

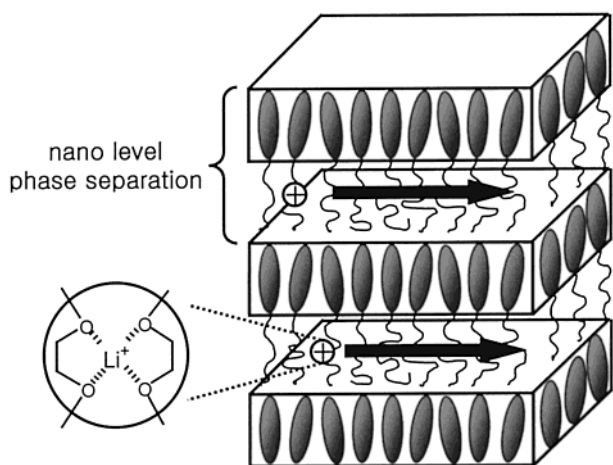
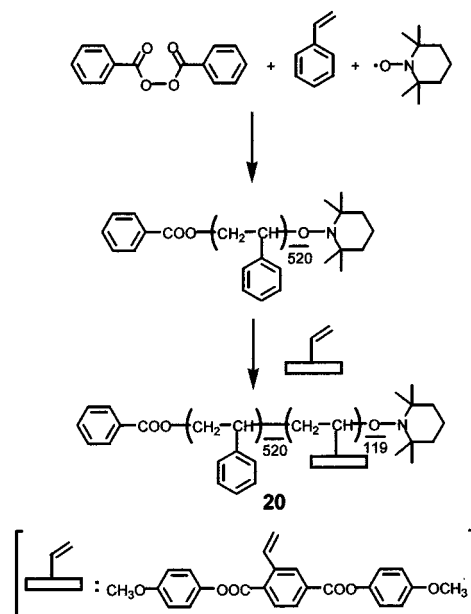


Figure 25. Schematic representation of Li^+ ion conduction for the complex of **19** with $[\text{Li}^+]/[\text{EO}] = 0.05$ in smectic A phase.

However, the conductivities decrease in the polydomain sample which disturbs the arrangement of ion paths. These results suggest that the self-organized rod–coil salt complexes can provide access to a novel strategy to construct ordered nanocomposite materials exhibiting low dimensional ionic conductivity.

Wu et al. reported on a rod–coil diblock copolymers based on mesogen-jacketed liquid crystalline polymer as the rod block and polystyrene as the coil block (Scheme 6).⁸² Styrene was polymerized by TEMPO mediated radical polymerization, followed by sequential polymerization of 2,5-bis[4-methoxyphenyl]oxycarbonylstyrene (MPCS) to produce the rod–coil diblock copolymer (**20**) containing 520 styrene and 119 MPCS repeating units. The rod–coil copolymer was observed to self-assemble into a core–shell nanostructure in a selective solvent for polystyrene

Scheme 6



block when the solution was cooled from 110 °C to room temperature as determined by a combination of static and dynamic laser light scattering studies. Interestingly, the average number of chains assembled in each nanostructure increases with the copolymer concentration in a selective solvent, different from the self-assembly of conventional diblock copolymers, whereas the size of the core remains a constant, very close to the contour length of the mesogen-jacketed rod block, but the shell becomes thicker (Figure 26). This observation may indicate

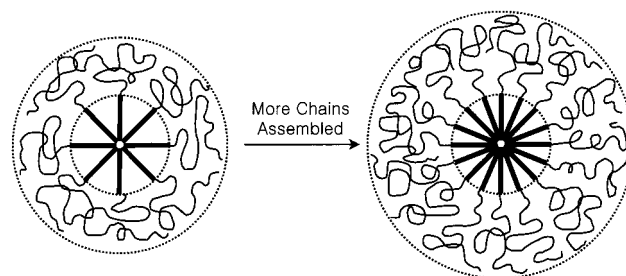


Figure 26. Schematic representation of a core–shell nanostructure formed by a self-assembly of **20** in a selective solvent.

that the attraction between the insoluble rigid-like mesogen-jacketed polymer blocks lead to their insertion into the core, while the repulsion between the soluble coil-like polystyrene blocks forces them to stretch at the interface.

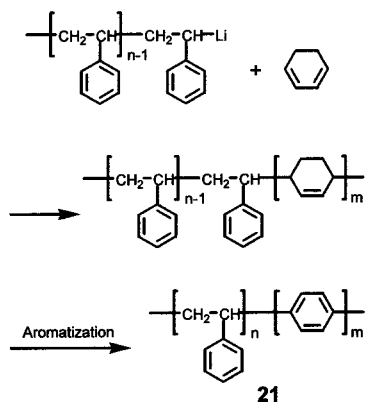
V. Rod–Coil Copolymers Based on Conjugated Rods

As a result of great interest in the optically and electronically active properties of highly conjugated and stiff rodlike molecules, a variety of oligomers and polymers have been synthesized to establish the molecular structure and property relationship.^{83,84} In addition to molecular structure, supramolecular structure was reported to have a dramatic effect on the

physical properties of conjugated rodlike molecules.^{85,86} Thus, manipulation of supramolecular structure in conjugated rods is of paramount importance to achieving efficient optophysical properties in solid-state molecular materials. One way to manipulate the supramolecular structure might be incorporation of the conjugated rod into a rod-coil molecular architecture which would allow formation of well-defined one-, two-, or three-dimensional conjugated domains in nanoscale dimensions. In this section, we will discuss on the studies of rod-coil systems based on well-defined conjugated rods. Synthetic strategies toward rod-coil copolymers involve either polymerization using a macroinitiator or grafting of two preformed conjugated blocks.

A monofunctionized segment may be used as macroinitiator to prepare rod-coil polymeric architecture as described Francois et al. (Scheme 7).⁸⁷⁻⁹³ The

Scheme 7



authors prepared polystyrene macroinitiator by living anionic polymerization. After sequential polymerization of styrene and then cyclohexadiene, a polystyrene-*block*-poly(cyclohexa-1,3-diene) was obtained and subsequently aromatized with *p*-chloranil to yield the corresponding oligo(*p*-phenylene) grafted to a polystyrene chain. Although the aromatization was not complete, the authors discovered special non-equilibrium honeycomb morphologies in which monodispersed pores arrange in a hexagonal array by evaporating the solvent from CS₂ solution in moist air (Figure 27). This novel morphology was proposed to be due to micelle formation. Interestingly, the presence of defects in the oligo(*p*-phenylene) sequence does not have a significant effect on honeycomb morphology. The authors also reported on the synthesis of polystyrene-polythiophene block and graft copolymers.⁹⁴⁻⁹⁷ These polymers incorporate the unique properties of polythiophene with processability. The reported block copolymers showed nearly the same spectral characteristics as pure polythiophene, and the authors proved that their block copolymers are still soluble after doping.

Rod-coil molecules containing structurally perfect conjugated rods were synthesized by using α -(phenyl)- ω -(hydroxymethyl phenyl)-poly(fluoren-2,7-ylene) as macroinitiator (Scheme 8).⁹⁸ Anionic polymerization of ethylene oxide by using the macroinitiator produced a corresponding rod-coil block copolymer (**22**). The absorption and emission measurements of

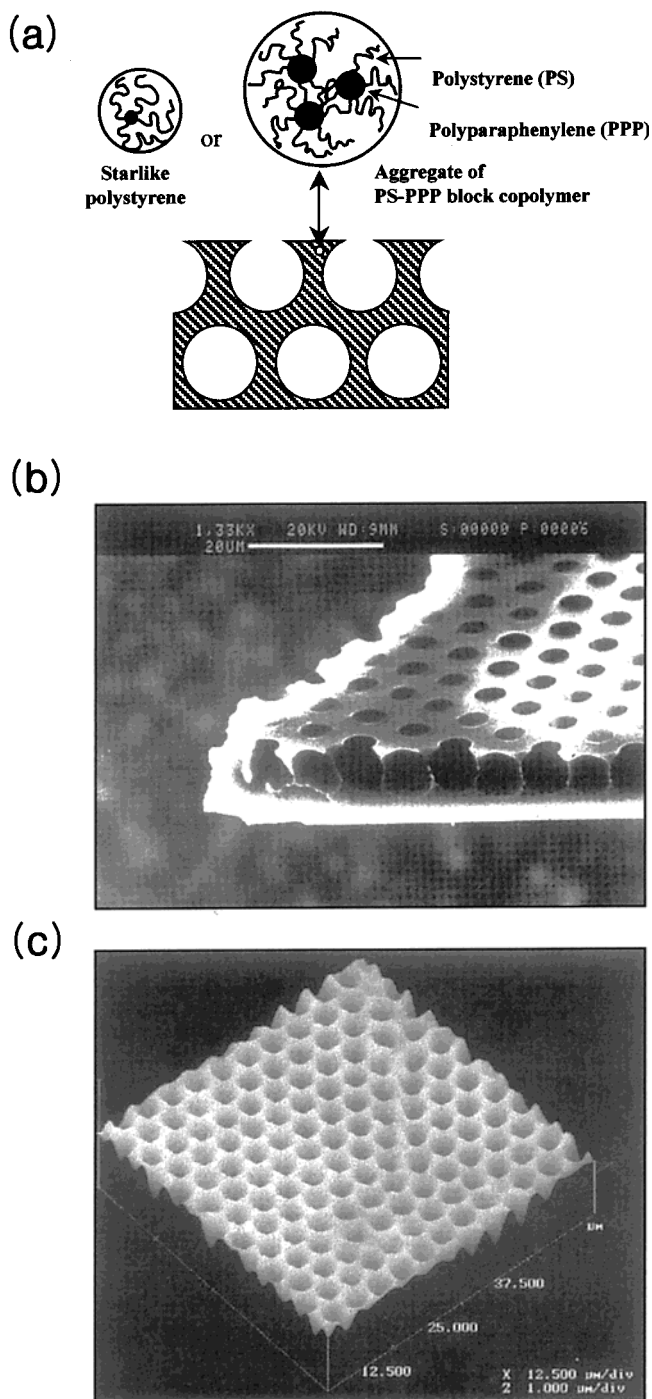
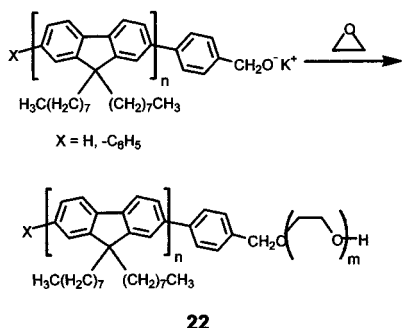


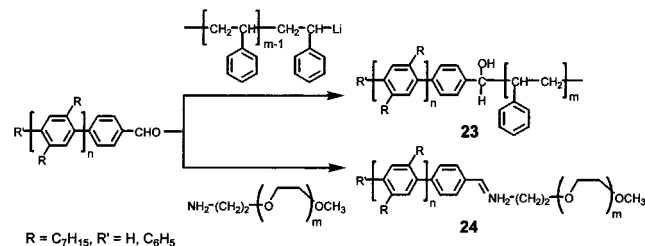
Figure 27. (a) Schematic representation for the cross section, (b) SEM image, and (c) AFM image of a honeycomb structure with a regular micropore in rod-coil copolymer **21**. (Reprinted with permission from Nature (<http://www.nature.com>), ref 93. Copyright 1994 Macmillan Magazines Ltd.).

this rod-coil copolymer revealed the influence of the coil blocks on the optoelectronic properties of the rod segments. The coupling reaction of preformed rod and coil blocks was also used to prepare a rod-coil block copolymer. Müllen et al. prepared perfectly end-functionalized oligo(2,5-diheptyl-*p*-phenylenes) (Scheme 9).⁹⁹ Further reaction of the end functionalized rod with either polystyrene or poly(ethylene oxide) yielded corresponding luminescent rod-coil block copolymers (**23** and **24**, respectively). Rod-coil copolymers consisting of poly(*p*-phenyleneethynylene) as the rod

Scheme 8



Scheme 9



block and poly(ethylene oxide) as the coil block (**25**) were also synthesized by coupling reaction of mono-functionalized rod to poly(ethylene oxide) (Chart 7).¹⁰⁰ More recently, the synthesis of triblock poly(isoprene-*block-p*-phenyleneethynylene-*block*-isoprene) (**26**) was reported by Godt et al. by using hydroxy functionalized polyisoprene (Chart 7).¹⁰¹

Lazzaroni et al. showed that rod-coil copolymers containing poly(*p*-phenylene) or poly(*p*-phenylene-ethynylene) as the rod segments have a strong tendency to spontaneously assemble into stable ribbonlike fibrillar morphology when coated on mica substrate as evidenced by AFM images.¹⁰² The ribbonlike supramolecular structure was proposed that in the first observed layer, the conjugated segments are packed according to a head-to-tail arrangement with their conjugated system parallel to each other surrounded by coil segments (Figure 28). A similar ribbonlike morphology was also observed from rod-coil copolymers consisting of poly(*p*-phenylene) as the rod block and poly(methyl methacrylate) as the coil block.¹⁰³

Hempenius et al. reported on a polystyrene-oligothiophene-polystyrene triblock rod-coil copolymer (Scheme 10).¹⁰⁴ The authors employed a polystyrene with a phenolic terminus that was modified

Chart 7

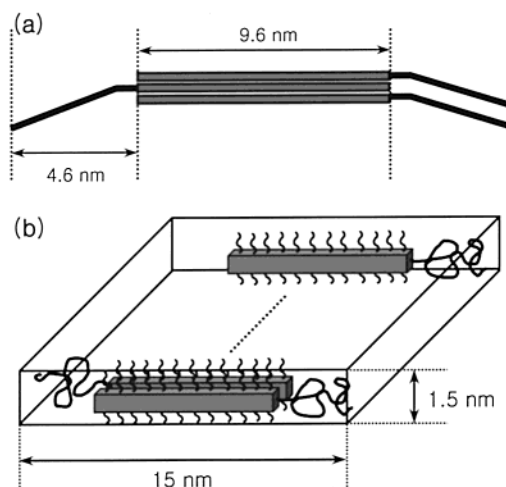
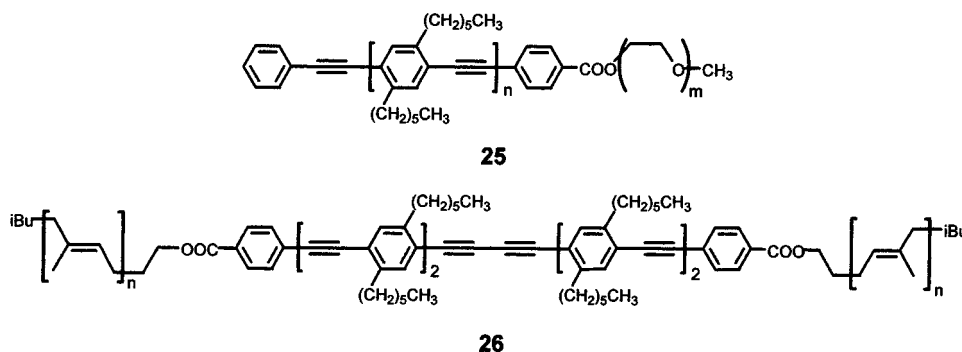


Figure 28. (a) Schematic molecular arrangement of three head-to-tail PPE-*block*-PDMS. (b) Schematic representation of the ribbonlike supramolecular structure formed by PPE-*block*-PDMS.

by an α -terthiophene unit, followed by a coupling reaction to yield a well-defined rod-coil triblock copolymer (**27**). Scanning force microscopy (SFM) revealed the formation of nonspherical micelles with axes of about 10 and 14 nm, corresponding to an aggregate of about 60 rod-coil molecules, consistent with the results determined from GPC (Figure 29). The optical properties were shown to be consistent with those of corresponding unsubstituted oligothiophenes.

Yu et al. reported on the synthesis of rod-coil block copolymers containing oligo(phenylene vinylene)s coupled to either polyisoprene (**28**) or poly(ethylene glycol) (**29**) (Chart 8).^{105,106} The first one was obtained by reaction of a living anionic polyisoprene derivative with oligo(phenylene vinylene)s containing an aldehyde group.¹⁰⁵ Four copolymers that have the same oligo(phenylene vinylene) block with different polyisoprene volume fractions were synthesized. TEM and small-angle X-ray scattering revealed alternating strips of rod-rich and coil-rich and coil-rich domains, and the domain sizes of the strips suggested that the supramolecular structures could be bilayer lamellar structure (Figure 30). On the other hand, it could be observed that as the conjugation length increases, the processability of the molecule decreases dramatically, thus limiting the length of the conjugated segment to be used in the coupling reaction. To solve the solubility problem, the authors modified the synthetic

Scheme 10

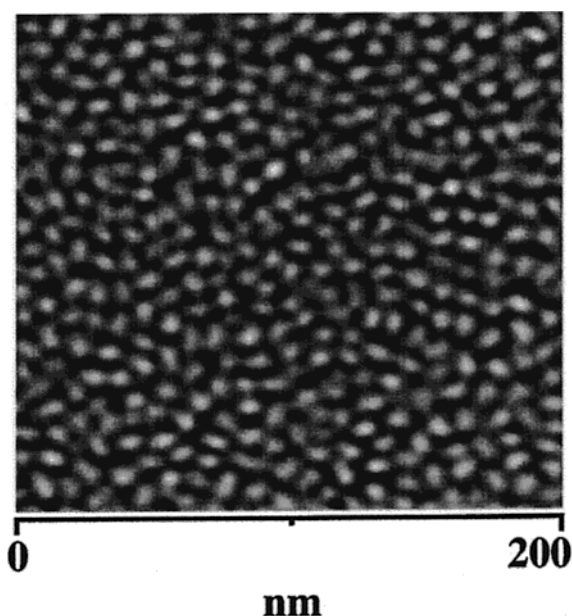
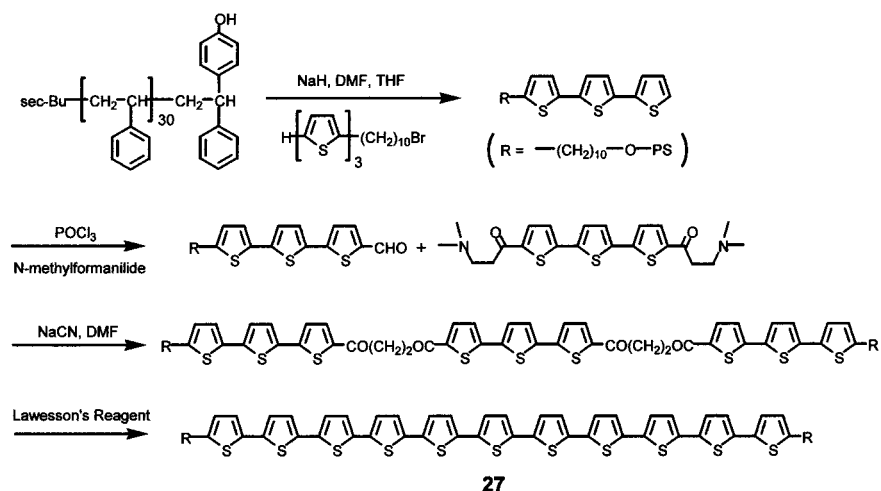
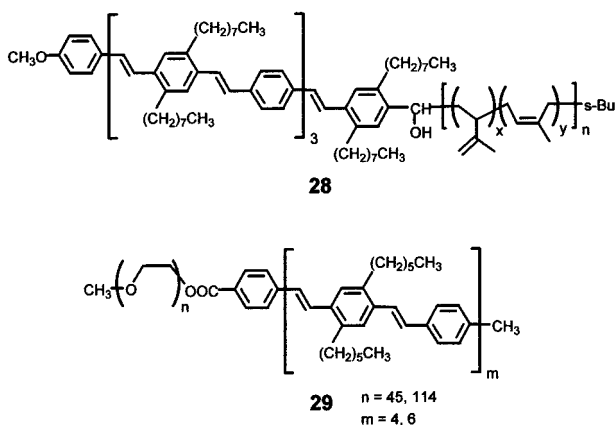


Figure 29. SFM image of nonspherical micelles formed by rod-coil triblock copolymer **27**. (Reprinted with permission from ref 104. Copyright 1998 American Chemical Society).

Chart 8



strategy by first coupling with poly(ethylene oxide) coil block with a oligo(phenylene vinylene) followed by coupling of the functionalized rod-coil copolymer.¹⁰⁶ The resulting block copolymer was subse-

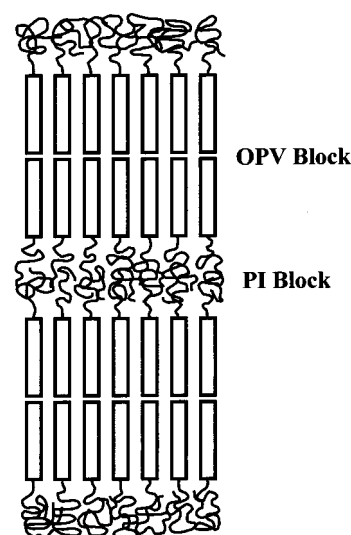


Figure 30. Proposed model for the bilayer structure of **28**.

quently coupled with oligo(phenylene vinylene) containing a vinyl end functional group to yield final rod-coil copolymers (**29**) with larger conjugated block (Chart 8). These rod-coil copolymers were observed to have remarkable self-assembling properties, and long cylindrical micelles are formed. TEM and AFM studies showed that the core of the micelles formed by **29** with $n = 45$ and $m = 6$ has a diameter of about 8–10 nm and is composed of a conjugated block surrounded by a poly(ethylene oxide) coil block (Figure 31).

Jenekhe et al. reported on the self-assembling behavior of rod-coil diblock copolymers consisting of poly(phenylquinoline) as the rod block and polystyrene as the coil block (Scheme 11).^{107,108} The rod-coil copolymers (**30**) were prepared by condensation reaction of ketone methylene-terminated polystyrene and 5-acetyl-2-aminobenzophenone in the presence of diphenyl phosphate. The degree of polymerization of the conjugated rod block in the rod-coil copolymers was controlled by the stoichiometric method. These block copolymers were found to self-assemble into fascinating supramolecular structures, although the rod block might not be monodisperse. For example, a rod-coil copolymer consisting of poly(phenylquino-

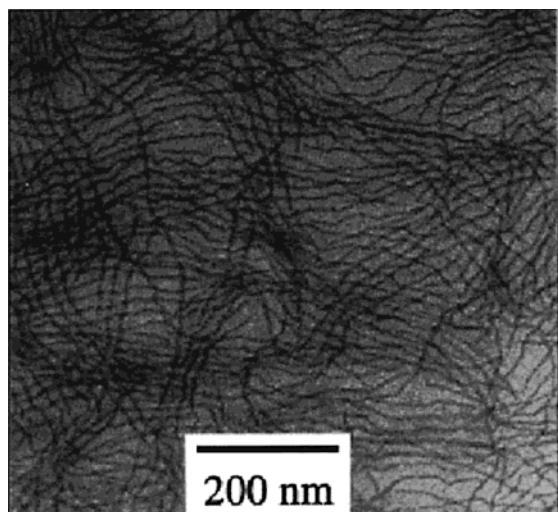
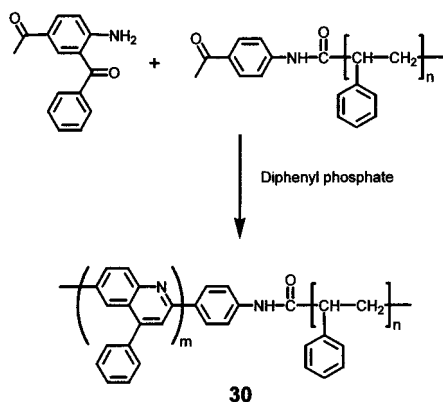


Figure 31. TEM image of long cylindrical micelles formed by **29** with $n = 45$ and $m = 6$. (Reprinted with permission from ref 106. Copyright 2000 American Chemical Society).

Scheme 11



line) with a degree of polymerization of 50 of polystyrene with degree of polymerization of 300 was observed to aggregate in the form of hollow spheres, lamellar, hollow cylinders, and vesicles in a selective solvent for the rod segment. The observed shape of supramolecular structures was dependent on the type of solvent mixture and drying rate. Photoluminescence emission and excitation studies showed that the photophysical properties strongly depend on the supramolecular structure of π -conjugated rod segments. Interestingly, their rod-coil systems proved to be possible for encapsulating fullerenes into the spherical cavities. As compared to conventional solvent for C_{60} , such as dichloromethane or toluene, the solubility is enhanced by up to 300 times when the molecules are encapsulated into micelles. In a further study, the authors observed that these rod-coil copolymers in a selective solvent for the coil segment self-assemble into hollow spherical micelles with diameters of a few micrometers, which subsequently self-organize into a 2-dimensional hexagonal superlattice (Figure 32).¹⁰⁹ Solution-cast micellar films were found to consist of multilayers of hexagonally ordered arrays of spherical holes whose diameter, periodicity, and wall thickness depend on copolymer molecular weight and block composition.

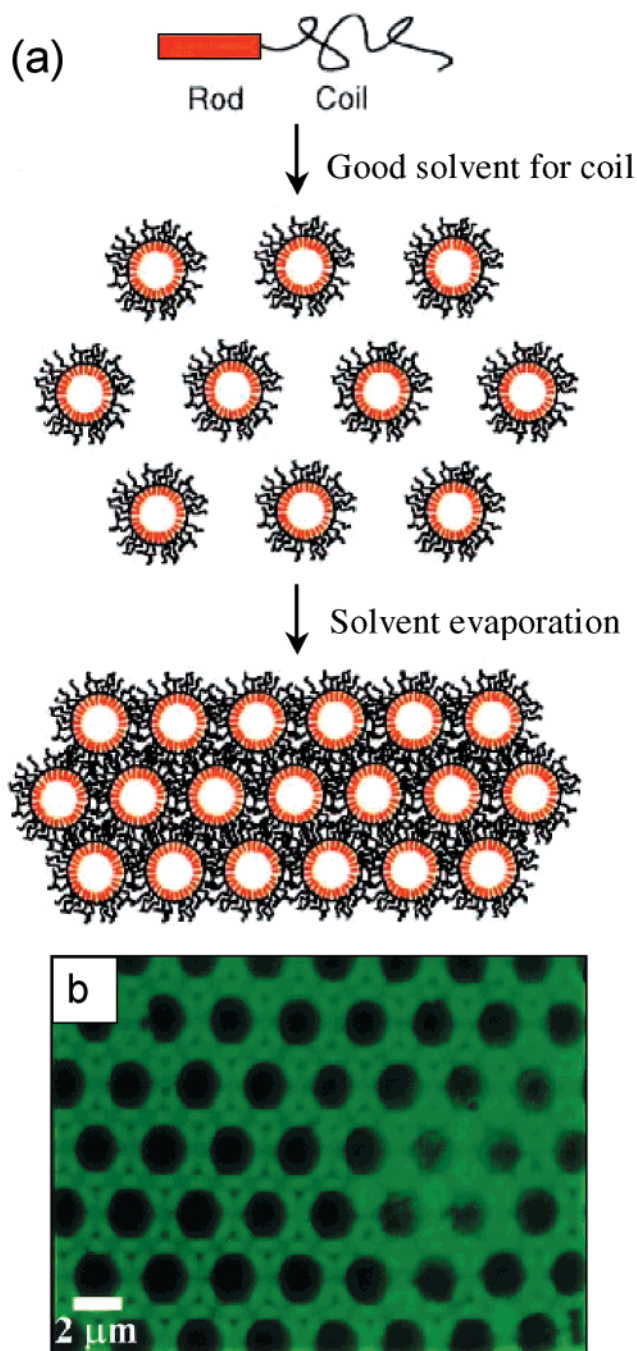


Figure 32. (a) Schematic representation of hierarchical self-organization of **30** into ordered microporous structure. (b) Fluorescence photomicrograph of solution-cast micellar film of **30** with $m = 10$ and $n = 300$. (Reprinted with permission from ref 109. Copyright 1999 American Association for the Advancement of Science).

The authors also reported on the supramolecular self-assembly from rod-coil-rod triblock copolymers prepared by copolymerization of 5-acetyl-2-aminobenzophenone with diacetyl functionalized polystyrene with low polydispersity (Scheme 12).¹¹⁰ In contrast to the rod-coil diblock copolymers which exhibit multiple morphologies, the triblock copolymers were found to spontaneously form only microcapsules or spherical vesicles in solution as evidenced by optical polarized, fluorescence optical, and scanning electron microscopies (Figure 33).

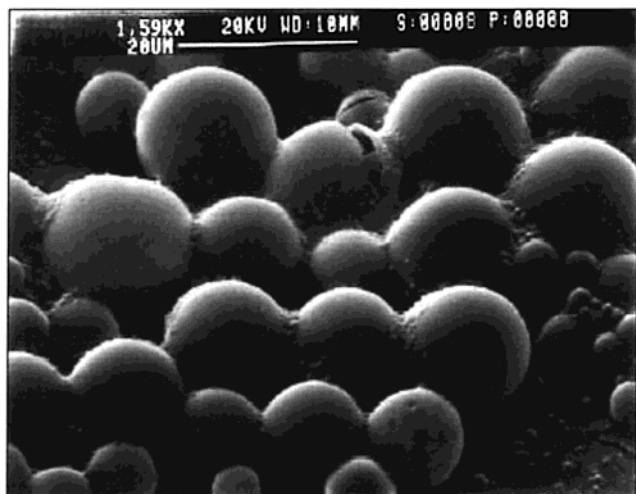
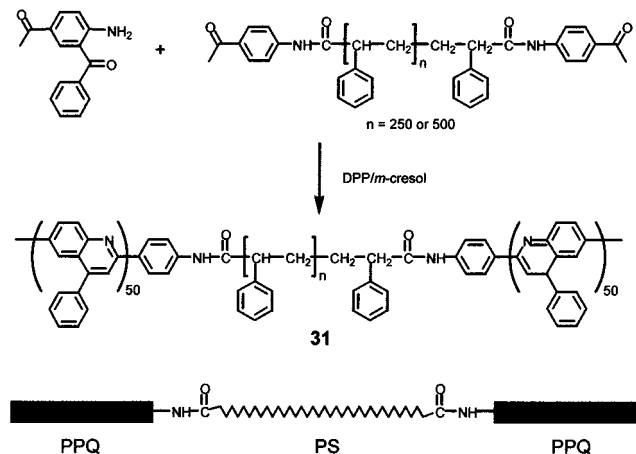


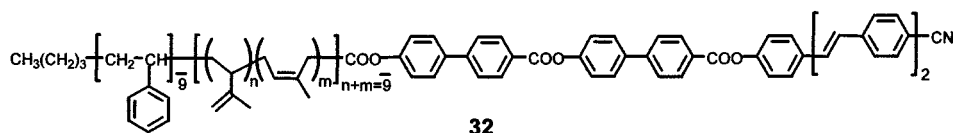
Figure 33. SEM image of microcapsules formed by **31** with $n = 250$. (Reprinted with permission from ref 110. Copyright 2000 American Chemical Society).

Scheme 12



As previously described, Stupp et al. reported on supramolecular materials formed by molecules with triblock architecture that self-organize into discrete mushroom-shaped nanostructures.^{58–60} To introduce optical functionalities, they synthesized rod–coil triblock molecules containing oligo(phenylene vinylene) (**32**) by reaction of functionalized rod–coil triblock molecules with hydroxy functionalized oligo(phenylene vinylene) building blocks (Chart 9).^{111,112} The cyano-substituted phenylene vinylene building block imparts fluorescence properties to these molecules and increases drastically their dipole moment. The nanostructured materials obtained contain thousands of molecular layers organized with polar ordering and give rise to strong photoluminescence. The authors also showed that supramolecular films composed of these dipolar rod–coil molecules self-organize into polar macroscopic materials showing piezoelectric activity.¹¹³

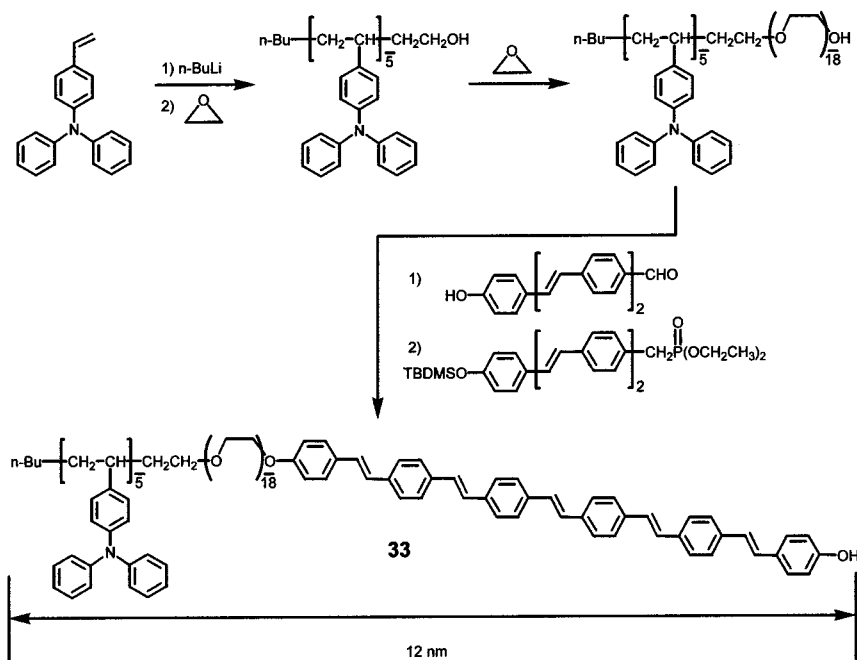
Chart 9



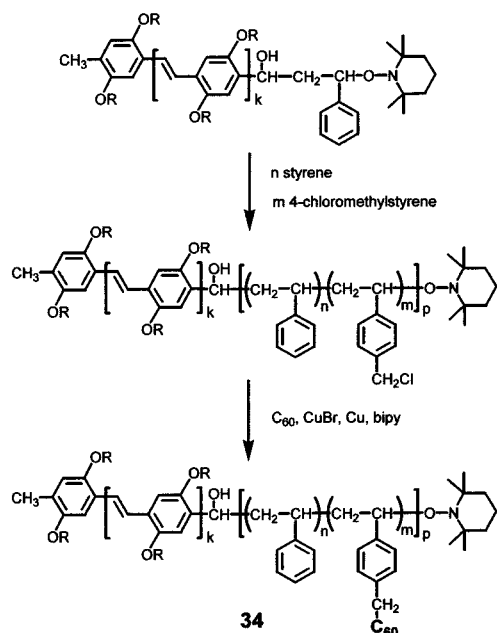
In addition, they have incorporated these supramolecular materials into triphenylamine moieties that are of interest as hole transport layers in light emitting devices.¹¹⁴ As shown in Scheme 13, living anionic polymerization of triphenylamine derivative followed by quenching with ethylene oxide afforded a hydroxy functionalized triphenylamine oligomer. The subsequent polymerization of this oligomer with ethylene oxide produced the diblock copolymer. Reaction of the resulting hydroxy terminated polymer with difunctionalized oligo(phenylene vinylene) produced a triblock copolymer endowed with an aldehyde functionality, which was further reacted with another oligo(phenylene vinylene) derivative with a Wittig–Horner reaction. Deprotection of the *tert*-butyl dimethylsilyl group yielded a triblock rod–coil copolymer containing a terminal hydroxy polar group (**33**). TEM revealed that these block molecules self-assemble into discrete nanostructures and electron diffraction indicated that this material contains crystalline domains with rod segments oriented perpendicular to the plane of the film, being both ethylene oxide segments and TPA segments contained in amorphous matrix. The emission spectra of **33** using 302 nm as the excitation wavelength showed substantial emission from conjugated rod segments and additional optical studies suggested that energy transfer occurs between the coil-like triphenylamine and rodlike conjugated segments of these molecules.

Hadziioannou et al. reported on the synthesis of a donor–acceptor, rod–coil diblock copolymer with the objective of enhancing the photovoltaic efficiency of the poly(phenylenevinylene)-C₆₀ system by incorporation of both components in a rod–coil molecular architecture that is self-assembling through microphase separation (Scheme 14).¹¹⁵ These rod–coil copolymers were obtained by using an end-functionalized rigid-rod block of poly(2,5-dioctyloxy-1,4-phenylene vinylene) as a macroinitiator for the nitroxide-mediated controlled radical polymerization of a flexible poly(styrene-stat-chloromethylstyrene) block. The chloromethyl group in the polystyrene block was subsequently transformed into C₆₀ onto the flexible polystyrene segment through atom transfer radical addition to yield the final rod–coil polymer (**34**) based on poly(phenylene vinylene) and C₆₀. Photoluminescence decay studies indicated that the luminescence from conjugated poly(phenylene vinylene) is quenched vigorously, suggesting efficient electron transfer as the donor–acceptor interface occurs. Films obtained through a coating process from CS₂ solution exhibit micrometer-scale, honeycomb-like aggregation structure (Figure 34). The porous character of the rod–coil materials was reported to be used as a template for the formation of a two-dimensional hexagonal array of functional dots.^{116,117}

Scheme 13



Scheme 14



VI. Conclusions

There is no doubt that manipulation of supramolecular architectures of rodlike polymers and their low molar mass homologues is of critical importance to achieving desired functions and properties in molecular materials. The incorporation of different rodlike segments such as helical rods, low molar mass mesogenic rods and conjugated rods as a part of the main chain in rod-coil molecular architecture has already proven to be an effective way to manipulate supramolecular structures in nanoscale dimensions. Depending on the relative volume fraction of rigid and flexible segments, and the chemical structure of these segments, rod-coil copolymers and their low molar mass homologues self-assemble into a variety of supramolecular structures through the combina-

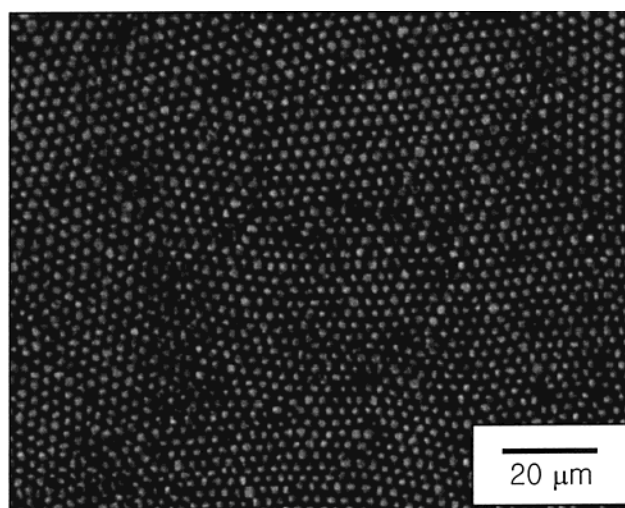


Figure 34. Optical transmission micrograph of honeycomb structures formed by **34**. (Reprinted with permission from ref 115. Copyright 2000 American Chemical Society).

tion of shape complementarity and microphase separation of rod and coil segments as an organizing force. The supramolecular structures assembled by rod segments in rod-coil systems include sheets, cylinders, finite nanostructures, and even perforated sheets that organize into 1-D, 2-D, and 3-D superlattices, respectively. It should be noted that self-assembly can be used to prepare well-defined macromolecular nano-objects that are not possible to prepare by conventional synthetic methodologies, when the rod-coil copolymers self-assemble into discrete supramolecular structures.

Another remarkable feature of rod-coil copolymers is their amphiphilic characteristics that show the tendency of their lipophilic and lipophobic parts to segregate in space into distinct microdomains. Depending on the solvent content and polarity, rod-coil copolymers self-assemble into a wide variety of different supramolecular structures. Because of the

covalent linkage of the amphiphilic segments, segregation does not lead to macroscopic separation. Instead, it results in the formation of different regions which are separated by interfaces at a molecular scale. This amphiphilic feature allows rod-coil copolymers to construct low dimensional ionic conductive nanomaterials as well as ordered nanocomposite materials.

It would be of interest to synthesize rod-coil copolymers based on conjugated rods that can self-assemble into a variety of supramolecular structures with unique optical and electronic properties because manipulation of supramolecular structures with different functionalities is of paramount importance to achieving desired physical properties of molecular materials. In this respect, many synthetic strategies have been developed that allow the incorporation of functional rod segments in well-defined rod-coil architectures for specific properties. Electron transfer, second harmonic generation, and piezoelectricity have been reported for supramolecular structures of rod-coil copolymers containing conjugated rods or highly polar end groups.^{59,111,113-115} Many more rod-coil systems are expected to be developed soon for possible applications as diverse as molecular materials for nanotechnology, supramolecular reactor, periodic porous materials, transport membrane, and biomimic materials.

VII. Acknowledgments

We gratefully acknowledge the financial support by CRM-KOSEF (2001), Korea Science and Engineering Foundation (R03-2001-00034), and the BK 21 fellowship (CBK).

VIII. References

- Whitesides, G. M.; Mathias, J. P.; Seto, C. P. *Science* **1991**, *254*, 1312.
- Lehn, J. M. *Supramolecular Chemistry*; VCH: Weinheim, Germany, 1995.
- Muthukumar, M.; Ober, C. K.; Thomas, E. L. *Science* **1997**, *277*, 1225.
- Föster, S.; Antonietti, M. *Adv. Mater.* **1998**, *10*, 195.
- Israelachvili, J. N. *Intermolecular and Surface Forces*; Academic Press: London, 1992.
- Collings, P. J.; Hird, M. *Introduction to Liquid Crystals*; Taylor & Francis: London, 1997.
- Stegemeyer, H. *Liquid Crystals*; Springer: New York, 1994.
- Bates, F. S.; Fredrickson, G. H. *Annu. Rev. Phys. Chem.* **1990**, *41*, 525.
- Hashimoto, T.; Shibayama, M.; Kawai, H. *Macromolecules* **1983**, *16*, 1093.
- Helfand, E.; Wasserman, Z. R. *Macromolecules* **1980**, *13*, 994.
- Leibler, L. *Macromolecules* **1980**, *13*, 1602.
- Semenov, A. N.; Vasilenko, S. V. *Sov. Phys. JETP S. V.* **1986**, *63* (1), 70.
- Semenov, A. N. *Mol. Cryst. Liq. Cryst.* **1991**, *209*, 191.
- Semenov, A. N.; Subbotin, A. V. *Sov. Phys. JETP A. V.* **1992**, *74* (4), 690.
- Williams, D. R. M.; Fredrickson, G. H. *Macromolecules* **1992**, *25*, 3561.
- Stupp, S. I. *Curr. Opin. Colloid Interface Sci.* **1998**, *3*, 20.
- Mao, G.; Ober, C. K. *Handbook of Liquid Crystals-Vol. 3: High Molecular Weight Liquid Crystals*; Wiley-VCH: Weinheim, 1998.
- Gallot, B. *Prog. Polym. Sci.* **1996**, *21*, 1035.
- Loos, K.; Munoz-Guerra, S. *Supramolecular Polymers-Chapter 7: Microstructure and Crystallization of Rigid-Coil Comblike Polymers and Block Copolymers*; Marcel Dekker: New York, 2000.
- Hamley, I. W.; Koppi, K. A.; Rosedale, J. H.; Bates, F. S.; Almdal, K.; Mortensen, K. *Macromolecules* **1993**, *26*, 5959.
- Hajduk, D. A.; Harper, P. E.; Gruner, S. M.; Honecker, C. C.; Kim, G.; Thomas, E. L.; Fetters, L. J. *Macromolecules* **1994**, *27*, 4063.
- Bates, F. S.; Schulz, M. F.; Khandpur, A. K.; Förster, S.; Rosedale, J. H.; Almdal, K.; Mortensen, K. *Faraday Discuss., Chem. Soc.* **1994**, *98*, 7.
- Khandpur, A. K.; Förster, S.; Bates, F. K.; Hamley, I. W.; Ryan, A. J.; Bras, W.; Almdal, K.; Mortensen, K. *Macromolecules* **1995**, *28*, 8796.
- Fredrickson, G. H.; Liu, A. J.; Bates, F. S. *Macromolecules* **1994**, *27*, 2503.
- (a) Matsen, M. W.; Schick, M. *Macromolecules* **1994**, *27*, 4014. (b) Milner, S. T. *Macromolecules* **1994**, *27*, 2333.
- Vavasour, J. D.; Whitmore, M. D. *Macromolecules* **1993**, *26*, 7070.
- Matsen, M. W.; Bates, F. S. *J. Polym. Sci. B: Polym. Phys.* **1997**, *35*, 945.
- Onsager, L. *Ann. N. Y. Acad. Sci.* **1949**, *51*, 627.
- Flory, P. J. *J. Chem. Phys.* **1949**, *17*, 303.
- de Gennes, P. G.; Prost, J. *The Physics of Liquid Crystals*, 2nd ed.; Oxford University Press: New York, 1993.
- Demus, D.; Goodby, J.; Gray, G. W.; Spiess, H. W.; Vill, V. *Handbook of Liquid Crystals, Vol. 1: Fundamentals*; Wiley-VCH: New York, 1998.
- Meier, D. J. *J. Polym. Sci.* **1969**, *C26*, 81.
- Matsen M. W.; Bates F. S. *Macromolecules* **1996**, *29*, 1091.
- Müller, M.; Schick, M. *Macromolecules* **1996**, *29*, 8900.
- Matsen, M. W.; Barrett, C. J. *Chem. Phys.* **1998**, *109*, 4108.
- Halperin, A. *Europhys. Lett.* **1989**, *10*, 549.
- Halperin, A. *Macromolecules* **1990**, *23*, 2724.
- Raphael, E.; de Gennes, P. G. *Makromol. Symp.* **1992**, *62*, 1.
- Zhang, G.; Fournier, M. J.; Mason, T. L.; Tirrell, D. A. *Macromolecules* **1992**, *25*, 3601.
- Yu, S. M.; Conticello, V. P.; Zhang, G.; Kayser, C.; Fournier, M. J.; Mason, T. L.; Tirrell, D. A. *Nature* **1999**, *399*, 167.
- Perly, B.; Douy, A.; Gallot, B. *Makromol. Chem.* **1976**, *177*, 2569.
- Billot, J.-P.; Douy, A.; Gallot, B. *Makromol. Chem.* **1977**, *178*, 1641.
- Douy, A.; Gallot, B. *Polymer* **1987**, *28*, 147.
- Klok, H.-A.; Langenwalter, J. F.; Lecommandoux, S. *Macromolecules* **2000**, *33*, 7819.
- Berger, M. N. *J. Macromol. Sci. Rev. Macromol. Chem.* **1973**, *C9* (2), 269.
- Bur, A. J.; Fetters, L. J. *Chem. Rev.* **1976**, *76* (6), 727.
- Fetters, L. J.; Yu, H. *Macromolecules* **1971**, *4*, 385.
- Aharoni, S. M. *Macromolecules* **1979**, *12*, 94.
- Aharoni, S. M.; Walsh, E. K. *Macromolecules* **1979**, *12*, 271.
- Aharoni, S. M. *J. Polym. Sci., Polym. Phys. Ed.* **1980**, *18*, 1439.
- Chen, J. T.; Thomas, E. L.; Ober, C. K.; Hwang, S. S. *Macromolecules* **1995**, *28*, 1688.
- Chen, J. T.; Thomas, E. L.; Ober, C. K.; Mao, G. *Science* **1996**, *273*, 343.
- Thomas, E. L.; Chen, J. T.; O'Rourke, M. J.; Ober, C. K.; Mao, G. *Macromol. Symp.* **1997**, *117*, 241.
- Wu, J.; Pearce, E. M.; Kwei, T. K. *Macromolecules* **2001**, *34*, 1828.
- Radzilowski, J. L.; Wu, J. L.; Stupp, S. I. *Macromolecules* **1993**, *26*, 879.
- Radzilowski, J. L.; Stupp, S. I. *Macromolecules* **1994**, *27*, 7747.
- Radzilowski, J. L.; Carragher, B. O.; Stupp, S. I. *Macromolecules* **1997**, *30*, 2110.
- Stupp, S. I.; Lebonheur, V.; Walker, K.; Li, L. S.; Huggins, K. E.; Keser, M.; Amstutz, A. *Science* **1997**, *276*, 384.
- Pralle, M. U.; Whitaker, C. M.; Braun, P. V.; Stupp, S. I. *Macromolecules* **2000**, *33*, 3550.
- Zubarev, E. R.; Pralle, M. U.; Li, L.; Stupp, S. I. *Science* **1999**, *283*, 523.
- Zubarev, E. R.; Pralle, M. U.; Sone, E. D.; Stupp, S. I. *J. Am. Chem. Soc.* **2001**, *123*, 4105.
- Lee, M.; Oh, N.-K. *J. Mater. Chem.* **1996**, *6*, 1079.
- Lee, M.; Oh, N.-K.; Zin, W.-C. *Chem. Commun.* **1996**, 1788.
- Lee, M.; Cho, B.-K.; Kim, H.; Zin, W.-C. *Angew. Chem., Int. Ed.* **1998**, *37*, 638.
- Lee, M.; Cho, B.-K.; Kim, H.; Yoon, J.-Y.; Zin, W.-C. *J. Am. Chem. Soc.* **1998**, *120*, 9168.
- Lee, M.; Cho, B.-K.; Ihn, K.-J.; Oh, N.-K.; Zin, W.-C. *J. Am. Chem. Soc.* **2001**, *123*, 4647.
- Lee, M.; Lee, D.-W.; Cho, B.-K.; Yoon, J.-Y.; Zin, W.-C. *J. Am. Chem. Soc.* **1998**, *120*, 13258.
- Lee, M.; Cho, B.-K.; Jang, Y.-G.; Zin, W.-C. *J. Am. Chem. Soc.* **2000**, *122*, 7449.
- (a) Lee, M.; Cho, B.-K.; Kang, Y.-S.; Zin, W.-C. *Macromolecules* **1999**, *32*, 7688. (b) Lee, M.; Cho, B.-K.; Kang, Y.-S.; Zin, W.-C. *Macromolecules* **1999**, *32*, 8531.
- Lee, M.; Cho, B.-K.; Oh, N.-K.; Zin, W.-C. *Macromolecules* **2001**, *34*, 1987.
- (a) Vilgis, T.; Halperin, A. *Macromolecules* **1991**, *24*, 2090. (b) Ji, S.-H.; Oh, N.-K.; Lee, M.; Zin, W.-C. *Polymer* **1997**, *38*, 4377.
- Thatcher, J. H.; Thanappasr, K.; Nagae, S.; Mai, S.-M.; Booth, C.; Owen, J. R. *J. Mater. Chem.* **1994**, *4*, 591.
- Le Nest, J. F.; Ghandini, A.; Schönenberger, C. *Trends Polym. Sci.* **1994**, *2*, 32.

- (74) Dias, F. B.; Voss, T. P.; Batty, S. V.; Wright, P. V.; Ungas, G. *Macromol. Rapid Commun.* **1994**, *15*, 961.
- (75) Percec, V.; Heck, J.; Johansson, G.; Tomazos, D.; Ungar, G. *Macromol. Symp.* **1994**, *77*, 237.
- (76) Lee, M.; Oh, N.-K.; Choi, M.-G. *Polym. Bull.* **1996**, *37*, 511.
- (77) Lee, M.; Oh, N.-K.; Lee, H.-K.; Zin, W.-C. *Macromolecules* **1996**, *29*, 5567.
- (78) Lee, M.; Cho, B.-K. *Chem. Mater.* **1998**, *10*, 1894.
- (79) Kang, Y. S.; Zin, W.-C.; Lee, D. W.; Lee, M. *Liq. Cryst.* **2000**, *27*, 2543.
- (80) Lee, M.; Jang, D.-W.; Kang, Y.-S.; Zin, W.-C. *Adv. Mater.* **1999**, *11*, 1018.
- (81) Ohtake, T.; Ogasawara, M.; Ito-Akita, K.; Nishina, N.; Ujie, S.; Ohno, H.; Kato, T. *Chem. Mater.* **2000**, *12*, 782.
- (82) Tu, Y.; Wan, X.; Zhang, D.; Zhou, Q.; Wu, C. *J. Am. Chem. Soc.* **2000**, *122*, 10201.
- (83) Kraft, A.; Grimsdale, A. C.; Holmes, A. B. *Angew. Chem., Int. Ed.* **1998**, *37*, 402.
- (84) Segura, J. L.; Martin, N. *J. Mater. Chem.* **2000**, *10*, 2403.
- (85) Osaheni, J. A.; Jenekhe, S. A. *J. Am. Chem. Soc.* **1995**, *117*, 7389.
- (86) Berresheim, A. J.; Müller, M.; Müllen, K. *Chem. Rev.* **1999**, *99*, 1747.
- (87) Zhong, X. F.; Francois, B. *Macromol. Chem. Rapid Commun.* **1998**, *9*, 411.
- (88) Zhong, X. F.; Francois, B. *Synth. Met.* **1989**, *29*, E35.
- (89) Zhong, X. F.; Francois, B. *Macromol. Chem.* **1990**, *191*, 2735.
- (90) Zhong, X. F.; Francois, B. *Macromol. Chem.* **1990**, *191*, 2743.
- (91) Zhong, X. F.; Francois, B. *Macromol. Chem.* **1991**, *192*, 2277.
- (92) Zhong, X. F.; Francois, B. *Synth. Met.* **1991**, *41*, 955.
- (93) Widawski, G.; Rawiso, M.; Francois, B. *Nature* **1994**, *369*, 387.
- (94) Francois, B.; Pitois, O.; Francois, J. *Adv. Mater.* **1995**, *7*, 1041.
- (95) Olinga, T.; Francois, B. *Macromol. Chem. Rapid Commun.* **1991**, *12*, 575.
- (96) Olinga, T.; Francois, B. *J. Chim. Phys., Phys. Chim. Biol.* **1992**, *89*, 1079.
- (97) Francois, B.; Olinga, T. *Synth. Met.* **1993**, *57*, 3489.
- (98) Marsitzky, D.; Klapper, M.; Müllen, K. *Macromolecules* **1999**, *32*, 8685.
- (99) Marsitzky, D.; Brand, T.; Geerts, Y.; Klapper, M.; Müllen, K. *Macromol. Rapid Commun.* **1998**, *19*, 385.
- (100) Francke, V.; Räder, H. J.; Müllen, K. *Macromol. Rapid Commun.* **1998**, *19*, 275.
- (101) KuKula, H.; Ziener, U.; Shöps, M.; Godt, A. *Macromolecules* **1998**, *31*, 5160.
- (102) Leclere, P.; Calderone, A.; Marsitzky, D.; Francke, V.; Geerts, Y.; Müllen, K.; Bredas, J. L.; Lazzaroni, R. *Adv. Mater.* **2000**, *12*, 1042.
- (103) Leclere, P.; Parente, V.; Bredas, J. L.; Francois, B.; Lazzaroni, R. *Chem. Mater.* **1998**, *10*, 4010.
- (104) Hempenius, M. A.; Langeveld-Voss, B. M. W.; van Haar, J. A. E. H.; Janssen, R. A. J.; Sheiko, S. S.; Spatz, J. P.; Möller, M.; Meijer, E. W. *J. Am. Chem. Soc.* **1998**, *120*, 2798.
- (105) Li, W.; Wang, H.; Yu, L.; Morkved, T. L.; Jaeger, H. M. *Macromolecules* **1999**, *32*, 3034.
- (106) Wang, H.; Wang, H. H.; Urban, V. S.; Littrell, K. C.; Thiyagarajan, P.; Yu, L. *J. Am. Chem. Soc.* **2000**, *122*, 6855.
- (107) Jenekhe, S. A.; Chen, X. L. *Science* **1998**, *279*, 1903.
- (108) Chen, X. L.; Jenekhe, S. A. *Langmuir* **1999**, *15*, 8007.
- (109) Jenekhe, S. A.; Chen, X. L. *Science* **1999**, *283*, 372.
- (110) Chen, X. L.; Jenekhe, S. A. *Macromolecules* **2000**, *33*, 4610.
- (111) Tew, G. N.; Li, L.; Stupp, S. I. *J. Am. Chem. Soc.* **1998**, *120*, 5601.
- (112) Tew, G. N.; Pralle, M. U.; Stupp, S. I. *J. Am. Chem. Soc.* **1999**, *121*, 9852.
- (113) Pralle, M. U.; Urayama, K.; Tew, G. N.; Neher, D.; Wegner, G.; Stupp, S. I. *Angew. Chem., Int. Ed.* **2000**, *39*, 1486.
- (114) Tew, G. N.; Pralle, M. U.; Stupp, S. I. *Angew. Chem., Int. Ed.* **2000**, *39*, 517.
- (115) Stalmach, U.; de Boer, B.; Videlot, C.; van Hutten, P. F.; Hadziioannou, G. *J. Am. Chem. Soc.* **2000**, *122*, 5464.
- (116) de Boer, B.; Stalmach, U.; Nijland, H.; Hadziioannou, G. *Adv. Mater.* **2000**, *12*, 1581.
- (117) de Boer, B.; Stalmach, U.; Melzer, C.; Hadziioannou, G. *Synth. Met.* **2001**, *121*, 1541.

CR0001131